Investigation on the Efficiency of Back-Contact Monocrystalline Silicon Solar Cells in Low Concentration and Non-Homogenous Illumination

by

Ghazal SHERAFATI

THESIS PRESENTED TO ÉCOLE DE TECHNOLOGIE SUPÉRIEURE
IN PARTIAL FULFILLMENT FOR A MASTER'S DEGREE
WITH THESIS IN ELECTRICAL ENGINEERING
M. Sc. A.

MONTREAL, MARS 30, 2021

ÉCOLE DE TECHNOLOGIE SUPÉRIEURE
UNIVERSITÉ DU QUÉBEC

BOARD OF EXAMINERS

THIS THESIS HAS BEEN EVALUATED

BY THE FOLLOWING BOARD OF EXAMINERS

Mr. Ricardo Izquierdo, Thesis Supervisor
Department of Electrical Engineering, École de technologie supérieure

Mr. Sylvain Cloutier, President of the Board of Examiners
Department of Electrical Engineering, École de technologie supérieure

Mr. Bora Ung, Member of the jury
Department of Electrical Engineering, École de technologie supérieure

THIS THESIS WAS PRENSENTED AND DEFENDED

IN THE PRESENCE OF A BOARD OF EXAMINERS AND PUBLIC

MARS 18, 2021

AT ECOLE DE TECHNOLOGIE SUPERIEURE

ACKNOWLEDGMENT

Étude de l'efficacité des cellules solaires en silicium monocristallin à contact arrière lorsque éclairées par une illumination de faible concentration non homogène

Ghazal SHERAFATI

RÉSUMÉ

Les énergies renouvelables et en particulier les cellules solaires font l'objet d'un intérêt constant. Par conséquent, l'étude des paramètres qui influencent l'efficacité des cellules solaires ainsi que les méthodes permettant d'améliorer leurs performances est d'un grand intérêt. Parmi les paramètres possibles qui influencent l'efficacité de la cellule solaire, l'éclairage non uniforme est le plus fréquent, en particulier dans les systèmes de cellules solaires à concentration ; par conséquent, l'étude de l'influence de l'éclairage non uniforme sur la performance des cellules solaires est d'une grande valeur.

Dans cette thèse, une revue de la littérature sur le sujet des cellules solaires et en particulier sur l'éclairage non uniforme est donnée. La cellule solaire à contact arrière est modélisée à l'aide de COMSOL et les effets du dopage sur les paramètres de la cellule sont étudiés. Le modèle simulé est vérifié par la théorie dans différentes conditions d'intensité de la lumière. Ensuite, ce modèle est étudié sous un éclairage non homogène dans différents rapports de concentration et les résultats des simulations sont comparés aux travaux précédents. Des conclusions sont tirées de la simulation concernant les impacts d'un éclairage non uniforme sur l'efficacité de la cellule solaire en basse et haute concentration.

Une cellule solaire à contact arrière est caractérisée en laboratoire et les impacts de la zone illuminée sur les caractéristiques de la cellule sont étudiés. De plus, les effets de la température sur les paramètres de la cellule sont mesurés et comparés avec la théorie qui montre un bon accord. Une méthode permettant de générer un éclairage non uniforme ainsi que les mesures de la carte d'intensité résultante sont présentées. La cellule solaire est étudiée sous différents éclairages non uniformes, avec des éclairages moyens différents sur la cellule et les résultats sont comparés avec la théorie.

Sur la base des résultats de la simulation et des expériences, il est conclu que les effets de l'éclairage non uniforme sur l'efficacité de la cellule sont négligeables pour une faible concentration, avant d'atteindre la saturation alors que la température reste constante, sous contrôle. En ce qui concerne la concentration moyenne et élevée, l'effet de la température et la saturation qui se produit en raison d'un éclairage non uniforme, entraîne une baisse de l'efficacité de la cellule.

Mots-clés : Cellule solaire, Éclairage non uniforme, Concentration, Efficacité

Investigation on the efficiency of back-contact monocrystalline silicon solar cells in low concentration and non-homogenous illumination

Ghazal SHERAFATI

ABSTRACT

Renewable energy and in particular solar cells are the subject of a continued interest. Consequently, studying the parameters that influence the efficiency of the solar cells as well as methods to improve their performance is of great interest. Among the possible parameters that impact the efficiency of the solar cell, non-homogenous illumination occurs more frequently in particular in concentrating solar cell systems; therefore studying the influence of non-homogeneous illumination on the performance of the solar cells are of a great value.

In this thesis, a literature review on the subject of solar cells and in particular non-uniform illumination is given. The back-contact solar cell is modeled using COMSOL and the effects of doping on the parameters of the cell are being studied. The simulated model is verified by the theory in different light intensity. Afterwards this model is studied in non-homogenous illumination in different concentration ratios and the results of the simulations are compared with previous works. Conclusions are made based on the simulation about the impacts of non-uniform illumination on the efficiency of the solar cell in low and high concentration.

A back-contact solar cell is characterized in the laboratory and the impacts of the illuminated area on the characteristics of the cell are studied. Moreover, the temperature effects on the parameters of the cell are measured and compared with the theory which shows a good agreement. A method to generate non-uniform illumination as well as the measurements of the resulted intensity map is presented. The solar cell is studied in different non-uniform illumination, having different average illumination over the cell and the results are compared with the theory.

Based on the results from simulation and experiments, it is concluded that the effects of non-uniform illumination on the efficiency of the cell is negligible for low concentration, before reaching saturation while the temperature stays constant, in control. Regarding the medium and high concentration, both temperature effect and saturation which occurs due to non-uniform illumination, leads to drop in the efficiency of the cell.

Keywords: Solar cell, Non-uniform illumination, Concentration, Efficiency

TABLE OF CONTENTS

Page

XII

LIST OF TABLES

LIST OF FIGURES

Page

LIST OF ABREVIATIONS

1D	One Dimensional
2D	Two Dimensional
3D	Three Dimensional
BJ	Back-Junction
BSF	Back Surface Field
EWT	Emitter Wrap-Through
FF	Fill Factor
I	Current
IBC	Interdigitated Back Contact
Isc	Short-circuit current
J	Current density
Jsc	Short-circuit current density
k	Boltzmann's constant
LACIME	Telecommunications and Microelectronics Integration Laboratory
MWT	Metallization Wrap-Through
n	Ideality factor
PETG	Polyethylene Terephthalate Glycol-modified
Pin	Input Power
Ploss	Power Loss
Pmax	Maximum Power
q	Electronic charge
r	non-uniformity factor
Ravg	Average illumination
Rmax	Maximum illumination
Rmin	Minimum illumination
Rs	Series resistance
T	Temperature
V	Voltage
Voc	Open-circuit voltage

XX

Vph	Output voltage of photodiode
X	Concentration ratio in sun
η	Efficiency

LIST OF SYMBOLS AND UNITS OF MEASUREMENTS

K	Kelvin
kWh	kilowatt hour
m	meter
V	Volt
W	Watt
yr	year
˚C	Celsius
Ω	ohm

INTRODUCTION

Due to the increase in the population and rising demand for energy, as well as the drawbacks of fossil fuels, the renewable energy sources have become of a great interest. Among different types of environmental-friendly sources, solar energy is considered as an alternative for the current situation.

In order to increase the efficiency of the solar cells and generate more power, the concentrated photovoltaics are used to concentrate the sunlight. These systems allow concentrating the light to achieve more input power, which results in higher output power. The concentrated light that illuminates the solar cell sees different degrees of non-uniformity based on the concentration system. Therefore, studying the effects of the non-uniform illumination on the performance of the cell is of great interest.

In this thesis, the back-contact solar cell is selected as the case study under a non-uniform illumination, and the impact of non-uniformity is studied on the efficiency of the cell. To study these effects, a simulated model is presented and verified by the theory to predict the behavior of the cell in different illumination profiles and light intensities. To verify the results of the simulation experimentally, the sample solar cell is studied in the laboratory under different illumination patterns.

This thesis is divided into 4 chapters as presented as follows:

Chapter 1 presents brief literature review of the solar cells and the previous studies on the effects of the non-uniform illumination on the performance of the solar cell.

Chapter 2 is devoted to the simulation of the back-contact solar cell, by presenting a model which predicts the behavior of the solar cell in different light intensities, temperatures and illumination profiles.

Chapter 3 discusses the experiments which are done using back-contact solar cell in the laboratory, in standard 1 sun illumination and non-uniform illumination. This chapter contains a method to measure the light intensity and non-uniform illumination pattern, to study the effects of this non-uniformity on the efficiency of the solar cell.

Chapter 4 is dedicated to the comparison between the results of the theoretical model, COMSOL simulations and experimental results. This chapter is presented to highlight the accuracy of the simulated model in predicting the behavior of the solar cell.

Finally, a conclusion is given, this includes a summary of the previous sections as well as a presentation of potential future works.

CHAPTER 1

LITERATURE RIVIEW

1.1   Introduction

The significant growth of population in recent years as well as the drawbacks of using fossil fuels, bring attention to the importance of using environmentally friendly sources. Among different types of environmental-friendly sources, solar energy is considered as an alternative for the current situation; as the total sun radiation during a year exceeds the world's yearly energy consumption (Hosenuzzaman *et al.*, 2015). In Canada, the solar production potential varies in provinces due to weather and latitude differences. Saskatchewan ranks first by the potential of producing 1330 kWh per year (according to the size of the solar power system in kW) and Quebec ranks fourth by the potential of 1183 kWh/kW/yr. The map of solar power production potential in different regions of Canada is shown in Figure 1.1.
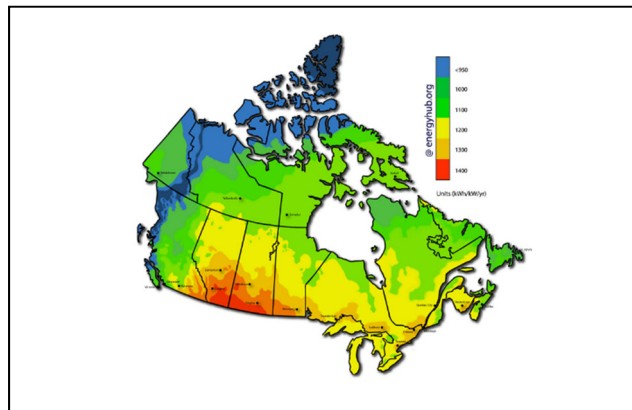
Figure 1.1 Solar production potential in Canada
Taken from Energyhub (2020)

Figure 1.2 shows the installed capacity of solar power in Canada from 2005 to 2018. This illustrates the fast development of the capacity of the solar cell as grew from a negligible production in 2005 up to 3040 MW in 2018. This fast development highlights the importance

4

of the solar power in Canada as well as the trend of current development which is a strong reason to study the solar power and ways to improve the performance of the solar cell.
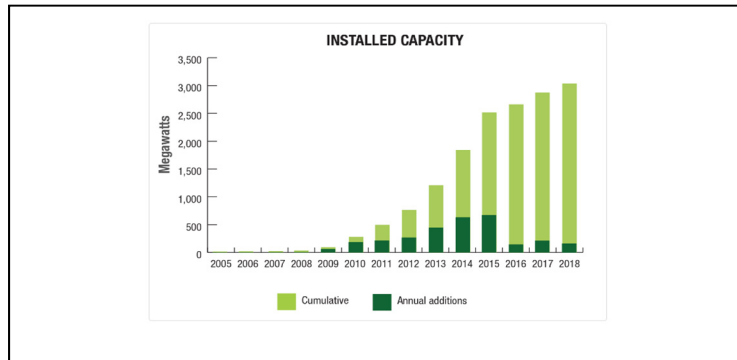
Figure 1.2 The capacity of solar cell industry in Canada
Taken from Natural Resources Canada (2020)

1.2   Operation of a solar cell

A solar cell is an energy converter, it converts light energy into electrical energy. The operation principle of a solar cell is quite simple and is based on the photovoltaic effect. A simplification of such effect is presented thereafter. When a solar cell is illuminated, photons randomly impact the surface, which in turns results in the creation of electrical carriers in the semiconductor. The produced electron-hole pairs are absorbed by metal contacts and the circulation of these pairs results in the electrical current. This simple process is illustrated in Figure 1.3, which shows a simple solar cell made of an antireflection coating, semiconductor base, emitter, and metal contacts. The cell is connected to an external load to allow the circulation of the generation carriers.
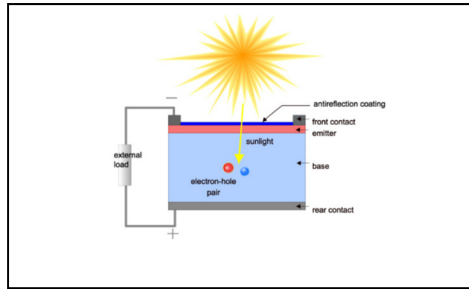
Figure 1.3 Schematic of a solar cell
under illumination
Taken from PVeducation (2020)

Due to their nature, the performance of a single-junction photovoltaic (PV) cell is similar to a diode, therefore in electrical simulations, the solar cell is modeled using diodes. Different combinations of diodes, current source, and resistors have been proposed to model solar cells, depending on the aspects which are of interests. The simplest electrical model of a solar cell uses a current source, one diode and two resistors: one in series and one in parallel which is named shunt resistor. This model is shown in Figure 1.4. This model is the most common model used to model solar cells, this is mainly due to its simplicity while providing accurate results (Jazayeri, Uysal et Jazayeri, 2013).
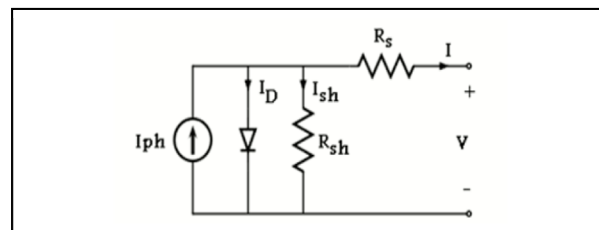
Figure 1.4 Single-diode model of a solar cell
Taken from Belkassmi *et al.* (2017)

1.2.1   Characteristics of the solar cell

To extract the characteristics of a solar, it is necessary to extract the IV curve. By applying different voltages to the cell and measuring the relevant current, the IV curve of the solar cell

is extracted. The IV curve reveals valuable information about the performance of the solar cell. Some important parameters which can be extracted from the IV curve are listed as below:

- Open-circuit voltage (Voc).
- Short-circuit current (Isc).
- Maximum power point (Pmax).

As an illustration, an IV-PV curve is shown in Figure 1.5. In this figure, the Isc, Voc, and the maximum power point on the IV curve are shown. By multiplying current and voltage, the PV curve is calculated and is shown on the same figure as the IV curve. The Pmax presents the point having maximum power and is shown at the peak of the PV curve.
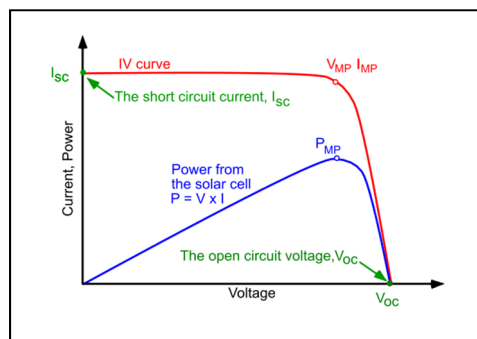
Figure 1.5 IV curve for a solar cell
Taken from PVeducation (2020)

The Fill Factor (FF) is a parameter that defines the quality of the solar cell. This parameter shows the ratio between maximum power produced by the cell and Voc times Jsc. This is shown in equation (1.1). The normal range of Fill Factor is normally between 40% and 60% and for some efficient solar cell it can reach up to 80-85%.

$$FF = \frac{Pmax}{Voc * Isc} \tag{1.1}$$

The efficiency of the solar cell (η) is calculated by dividing the produced maximum power of the cell by input power (Pin) as shown in equation (1.2). (Alharbi et Kais, 2015) explains the

theoretical limits of the solar cell's efficiency and presents 33.3% as the best possible efficiency for the single-junction PV at 300K.

$$\eta = \frac{Pmax}{Pin} \tag{1.2}$$

1.2.2 Overview of different types of solar cells

The general types of solar cells are Silicon-based, thin-film, organic, and advanced nano-PV. Among them, silicon-based cells are the most common types in the PV market due to the rich sources of silicon, simple fabrication process, and high conversion efficiency (Mat Desa *et al.*, 2016). Figure 1.6 shows the confirmed efficiency of different types of single-junction solar cells under standard test condition, using the data published in (Green *et al.*, 2020). Among them, the best efficiency is achieved using GaAs thin-film cells boasting the efficiency of 29.1%. On the second place, Silicon crystalline solar cells have a confirmed efficiency of 26.7%. The least efficient case is the organic solar cell by having the efficiency of just 13.5%.
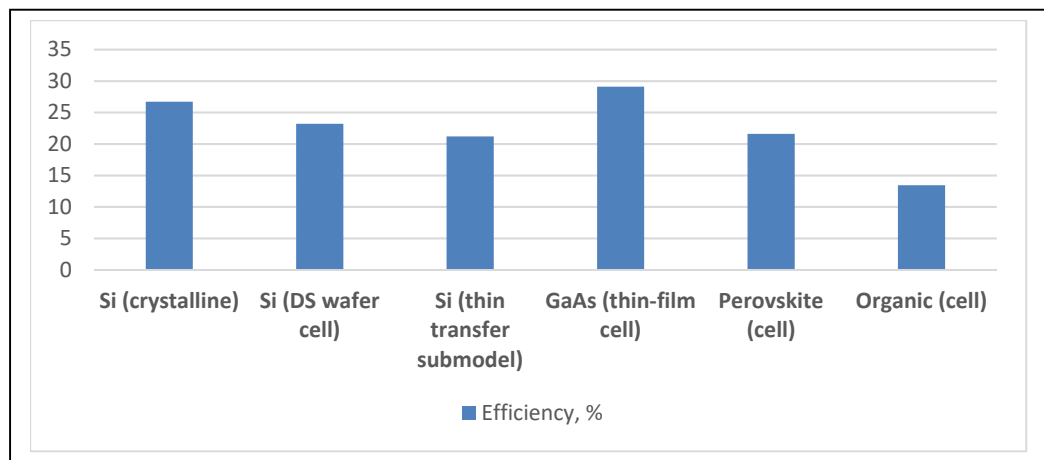
Figure 1.6 The confirmed efficiency of some solar cells
Taken from Green et al. (2020)

1.3   Conventional solar cell

In a conventional solar cell, shown in Figure 1.7, the metal grid of fingers and busbars are placed on the front surface. The emitter is located near the top surface as well. The back surface is normally fully covered by rear contact. In these types of solar cells, the thickness of the fingers and of the busbars plays an important role as the thicker they are, the more shadow on the front surface will be. This leads to a drop in the efficiency of the cell especially in concentrating systems. However, reducing the size of such contacts will also prove detrimental as thin contacts cause higher series resistance which then leads to lower efficiency (Kerschaver et Beaucarne, 2006). Therefore, an optimum thickness of fingers and busbars to provide an optimum operation of the cell is of a great value.
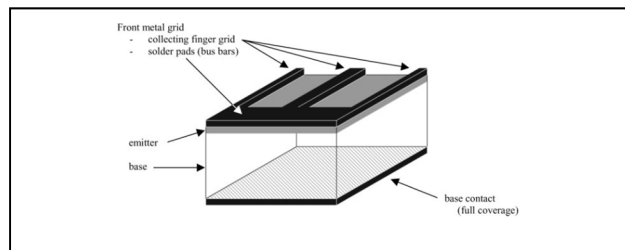
Figure 1.7 Schematic representation of a
conventional solar cell
Taken from Kerschaver et Beaucarne (2006)

1.4   Back-contact solar cells

According to (Kerschaver et Beaucarne, 2006) back-contact solar cells can be classified into 3 main categories: Metallization Wrap-Through (MWT), Emitter Wrap-Through (EWT), and Back-Junction (BJ) or Interdigitated Back Contact (IBC). For illustration purposes, the schematic of these three categories are shown in Figure 1.8.

The first category is the MWT, in such solar cells some parts of the front grid are located on the back side of the cell and the current passes through metal edges to the back contacts (Jooss *et al.*, 2000). The second category is EWT type solar cells, in such type of solar cells there is

no metal grid on the front and the emitter is located near the top surface (Van Kerschaver, De Wolf et Szlufcik, 2000). Finally, in the case of IBC solar cells, both emitter and metal grid are on the rear side, which leads to the elimination of shading losses.

The shading loss has a major influence on the efficiency of the solar cell especially in the case of concentrating solar cells. Therefore, back-contact solar cells are of a great interest in concentrating systems. Moreover, as the contacts are located on the rear side, the designers have more flexibility to choose wider fingers to have less resistance which in turns leads to better performance of the cell (Lammert et Schwartz, 1977).
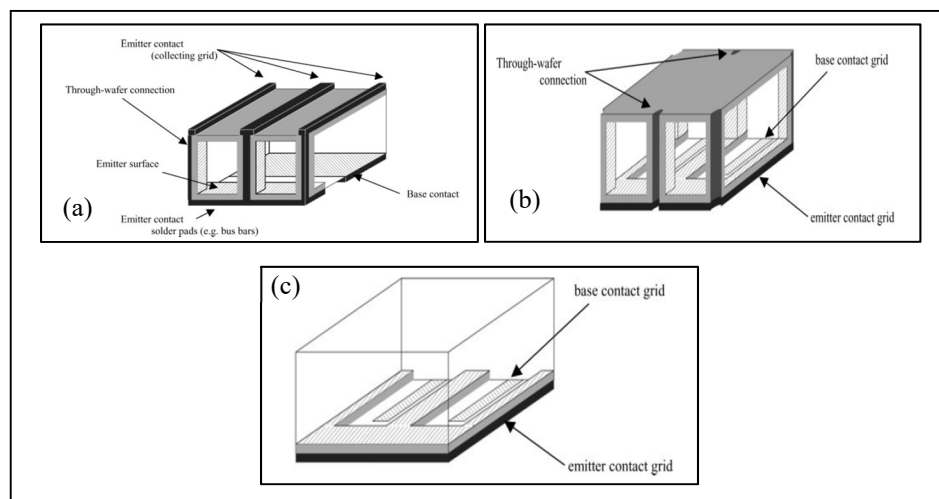
Figure 1.8 Schematic of (a) MWT (b) EWT and (c) BJ solar cell
Taken from Kerschaver et Beaucarne (2006)

Therefore using back contact solar cells is a solution to increase the performance of solar cells, as such the main advantages of these cells have been compiled by (López Rodríguez, 2016). Among these advantages, the following can be highlighted:

- No shading loss.
- Optical optimization on the front side while electrical optimization is on the back side.
- Decrease in series resistance.
- Appropriate for tandem solar cells.

- Facilitate the module's interconnections.

However, the use of back contact solar cells is not a perfect solution, as on the other hand, (López Rodríguez, 2016) showed that these cells have the following drawbacks:

- Need high quality silicon or thin wafer (the charge carriers near the surface should reach the back side).
- Need low surface recombination.
- Need high quality passivation at back side.
- Complicated fabrication.

1.5 Concentrators

As the generated power of the solar cell is proportional to the input power, increasing the input power of the solar cell will result in an increase output power of the solar cell. One of the ways to artificially increase the input power of the cell is to use concentrators to increase the light intensity which reaches the surface of the solar cell. This increase of the input power leads to higher generated current and voltages, which in turns results in slight improvements in the performance of the cell thus reducing the long-term cost.

The concentrators are presented based on their solar concentration in sun, which is defined as a unit equal to a light intensity of 1000 W/m^2. (Pérez-Higueras *et al.*, 2011) presents the classification of the concentrators based on the concentration ratios into low concentration (between 1 and 40 sun), medium concentration (between 40 and 300 sun) and high concentration (more than 300 sun).

There are different types of concentrators which can generate various concentration ratios. (Shanks, Senthilarasu et Mallick, 2016) presents the main types of concentrators as refractive, reflective, luminescent, and total internal reflection. These systems are described thereafter.

1.5.1 Refractive photovoltaic systems

Regarding refractive photovoltaic systems, the Fresnel lens is the most common, such a system is shown in Figure 1.9. These systems are largely used as a concentrator in refractive PV systems due to their small size and low weight and cost (Pan *et al.*, 2011); however, they have the limitation of producing up to 1000 suns due to the longitudinal chromatic aberration (Shanks, Senthilarasu et Mallick, 2016). (Languy et Habraken, 2013) proposes an improved lens to reduce the longitudinal chromatic aberration which in turns allows the illumination to reach up to 8500 sun.
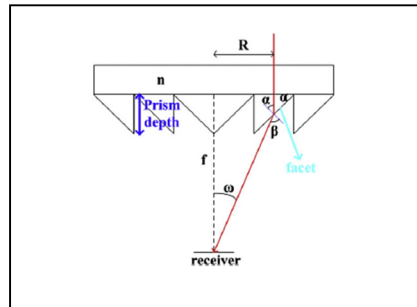
Figure 1.9 Schematic of a
Fresnel lens
Taken from Pan et al. (2011)

1.5.2 Reflective photovoltaic systems

Parabolic troughs are mainly used in reflective photovoltaic systems. These troughs allow achieving a concentration of up to 200 suns (Murphree, 2001). Using parabolic trough as a concentrator allows concentrating the light on the receiver, which is normally attached to cooling tubes to ensure a low temperature of operation. The schematic of a parabolic trough is shown in Figure 1.10, which illustrates the performance of the trough which concentrates the light beam on the receiver.
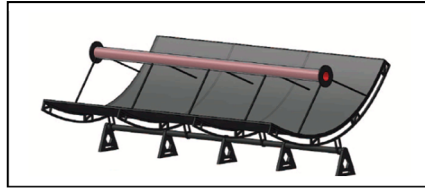
Figure 1.10 Schematic of a
parabolic trough
Taken from Basit *et al.* (2014)

1.5.3 Luminescent photovoltaic systems

In these systems, luminophores are coated on top of a glass sheet or within it. This allows using these systems in large scale in modern urban environment. The main part of this system is the luminophore, as it absorbs the photons and results in concentration of the incident light. The schematic representation of it is shown in Figure 1.11, taken from (Moraitis, Schropp et van Sark, 2018). The mechanism of this system consists of absorption of the light by luminescent and guidance of the re-emitted light to the solar cell, using trapping reflection systems.
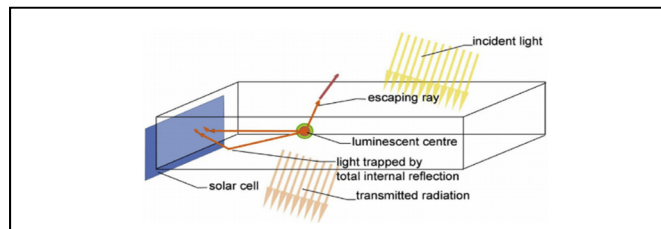
Figure 1.11 Schematic of a luminescent
photovoltaic system
Taken from Moraitis, Schropp et van Sark (2018)

1.5.4 Total internal reflection

Total internal reflection systems are based on reflection and refraction of rays, trapped in two neighboring pyramids and is shown in Figure 1.12. This system takes into account both reflective and refractive systems between two pyramids which results in concentrated light. The movement of rays between the pyramids are due to the textured surface which leads to better performance of the cell (Hamel, 2016).
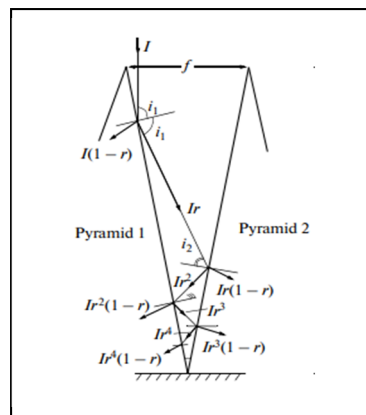
Figure 1.12 Mechanism of
total internal reflection
Taken from Hamel (2016)

Among different types of concentrators, the Fresnel lens and the parabolic trough have a line focus and they are more common in concentrating systems. In Table 1.1, some of the positive and negative points of these two concentrators are presented. This table is a compilation of the data presented by (Khamooshi *et al.*, 2014), (Basit *et al.*, 2014), and (Baharoon *et al.*, 2015). As it is summarized in this table, each of these two concentrators is appropriate for specific conditions based on the available physical space or the needed efficiency. The Fresnel lens is more common in smaller scales than parabolic trough; however, the Fresnel lens has the drawback of losing light on the draft facet and it is not on the optimum operation on the edges. On the other hand, parabolic trough is limited by direct radiation as well as low optical and quantum efficiency.

Table 1.1 Positive and negative points of Fresnel lens and Parabolic trough

	Advantages	**Disadvantages**	**First prototype**
Fresnel lens	Small volume Light weight Mass production	Not perfect on the edges Possibility of lost light	Genoa, Italy 1964
Parabolic trough	Efficient use of direct solar radiation Simple construction	Only direct radiation is used Low optical and quantum efficiency	Meadi, Egypt 1913

1.6   Non-homogenous illumination

Non-homogenous illumination is a common occurrence in PV systems. The reasons for this phenomenon are presented in Table 1.2 based on (Li *et al.*, 2018). These reasons are classified into 3 main categories. The first one is caused by the design of the concentrator which is the major reason for non-uniform illumination. The second one is the relative position of the cell and the sun. Finally, all the other factors such as shading and spectral response are joined together.

Table 1.2 Reasons for non-uniform illumination
Taken from Li *et al.* (2018)

Concentrator design	**Relative position of the solar cell and the sun**	**Other factors**
• Unreasonable design • Material • Profile errors • Manufacturing problems	• Improper tracking system • Deviation of optics and cell	• Shading • Spectral response

1.7　　Effects of non-homogenous illumination

Non-uniform illumination has an impact on the parameters of the solar cell. These impacts depend on different criteria such as the average illumination, the temperature and the type of solar cell. Moreover, the non-uniform illumination results in non-uniformity of the temperature of the solar cell which in turns results in changes in the characteristics of the solar cell.

Studies which have been performed in this filed are mainly focused on two scenarios:
- In the first one, the non-uniformity happens on a single cell.
- In the second scenario, the non-uniform illumination occurs on a series of cells.

(Pfeiffer et Bihler, 1982) presents a method to study the effects of non-uniform illumination on the generated power of Silicon solar cells under 9 sun illumination. The results show negligible loss in the output power in both cases. In (Luque, Sala et Arboiro, 1998), the effects of low concentrated non-uniform illumination on the efficiency of the Silicon cell is studied while considering the non-uniform temperature, which results in reduction in the efficiency. Moreover, the article highlights the negligible effects of the non-uniform illumination on the efficiency of the solar cell while keeping the temperature constant all over the cell at low temperature. (Mellor *et al.*, 2009) studies a Gaussian illumination pattern under 12 sun illumination and concludes that the impact of non-uniformity on the efficiency of the Silicon solar cell is dependent on the finger width. It is concluded that by choosing the optimum finger width for specific illumination pattern, the effects of non-uniformity are negligible. Regarding the location of non-uniform illumination on the Silicon solar cell, (Paul *et al.*, 2015) presents a method to cover the cell partially and study the effects on the efficiency of the cell. The results show minor effects on the characteristics of the cell. Moreover, the impact of non-uniformity on the efficiency of the cell is studied in low and medium energy flux, which shows the low sensitivity toward non-uniform illumination while having low concentration.

Regarding Multijunction solar cells, (Herrero *et al.*, 2012) studies the effects of non-uniform illumination up to 1000 sun for multijunction solar cells, and shows the high sensitivity of

these types of cells to the non-uniform illumination. (Sharma, 2017) studies the effects of non-uniform illumination as well as temperature changes on the efficiency of multijunction solar cells and shows the same trend as previous works in high concentration.

For the case having non-uniform illumination over several cells, the studies show high sensitivity to the non-uniform illumination in medium concentration, as presented in (Coventry, 2005). In this article, the experiments are done having non-uniform illumination over 28 solar cells connected in series, which results in major changes of the efficiency.

From this literature review, it can be concluded that the studies which are made show negligible changes in the efficiency due to non-uniform illumination in low concentration, while in medium and high concentration, the solar cell's performance decreases considerably due to both temperature effects and non-uniform illumination.

CHAPTER 2

SIMULATION

2.1 Introduction

Studying the effects of non-homogeneous illumination on the solar cell's characteristics is necessary to improve the performance of solar cells. This is particularly of interest in concentrated solar cells, due to the nature of concentrators which increase the non-homogeneity. Therefore, a simulated model that can represent the actual solar cell to study its behavior under non-homogeneous illumination is of a great value.

In this chapter, a basic model of the back-contact solar cell is presented and validated to simulate the behavior of the cell under non-homogenous illumination. The model is initially studied under uniform light intensity and its behavior is compared with the theory. Thereafter the influence of the temperature on the performance of the cells is studied. In the next step, non-uniform illumination patterns are considered to investigate their effects on the characteristics and more specifically on the efficiency of the cell.

2.2 Software

There are different approaches to simulate a solar cell, depending on the aspects needed to study. Different types of software are available to model the cell, from generic simulators like Simulink and COMSOL to programs which are specifically designed to model solar cells like SunSolve and Griddler. Considering the objective of this project, different types of software were tested to model our solar cell. A summary of the investigated software is shown in Table 2.1. This table highlights the main features of each program.

Table 2.1 Comparison of different software for the simulation of solar systems

Program	Features
Pspice	• For digital and analog circuits • Equivalent circuit with diodes for modeling PV
Simulink	• Solar block (equivalent circuit with 1 or 2 diodes)
COMSOL	• Modeling Semiconductor • Solar irradiation by entering latitude, longitude, date, and time data • Heat radiation
PV Lighthouse (SunSolve)	• Providing useful calculators • Defining silicon wafer and desired geometry and layers • Allows defining partial illumination
Griddler	• Designed for H-pattern metal grids • Integrates with AutoCAD to import designs
Homer Pro	• Can model two popular types of photovoltaic (PV) arrays: flat panel and concentrating • Not specifically designed for solar PV • Appropriate for solar irradiance simulation
PV F-Chart	• Weather data for over 300 locations • Weather data can also be added • Finite Element Heat Transfer (FEHT)
PV-Sol	• 2D solar software design tool for simulating photovoltaic system performance • Comes with Meteosyn climate data software; therefore, allows to add custom climate data • Financial analysis

All these programs have different features and uses. Some are more concentrated on the electrical modeling of solar cell such as Pspice and Simulink, others are more focused on defining the structure of solar cell such as SunSolve and Griddler. Some others, allow modeling the real implementation of PV systems, as they take into account the real data of climate and location such as PV F-Chart and PV-Sol.

The programs which are specifically designed to model solar cells are mostly limited to conventional solar cell's structure. Due to the specific structure of the solar cell under the study

(back contact) as well as the complexity of non-homogenous illumination, COMSOL has been selected as the simulation program.

COMSOL is a software that allows finite element analysis. This type of analysis can be applied to a wide range of physics to model the behavior of real-life structures. In this case, the semiconductor module allows modeling the physics of the solar cell by defining the material, the relevant characteristics and doping as well as the approach to study. Another benefit of using COMSOL is that it allows adding different physics such as a heat transfer interface for further analysis of the influence of the temperature on the performance of the solar cell.

In addition, COMSOL allows the modeling of the cell in 1D, 2D or for more complicated studies in 3D. Due to the objective of this thesis which is studying the effects of non-uniform illumination, a 3D model of the back-contact solar cell is selected as the representative of the actual solar cell.

2.3   Review of back-contact solar cell

As it is discussed in the first chapter, in back contact solar cells both metal contacts are located on the rear side of the cell and the carriers which are generated due to the illumination can be absorbed by BSF (back surface field) and Emitter on the back side of the cell. The simple structure of an IBC solar cell is shown in Figure 2.1, which is inspired from (Fell *et al.*, 2014). This structure contains moderate doped p-type silicon base, heavily doped BSF and heavily doped Emitter. The highly doped areas increase the separation of charge carriers and thus improve the performance of the cell.

20
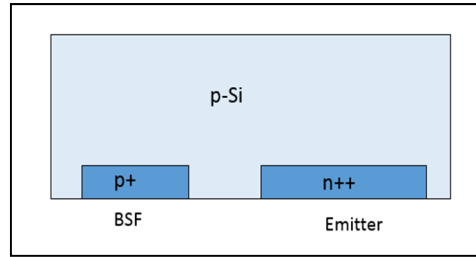
Figure 2.1 Basic structure of back-
contact solar cell

Low doping is generally defined as a doping inferior to 10^{14} per cm^3 while heavy doping is defined as doping superior to 10^{18} per cm^3, any doping in between these values is considered as a moderate doping. This is clearly indicated in Figure 2.2, which presents the ranges for low doping to heavy doping in silicon.
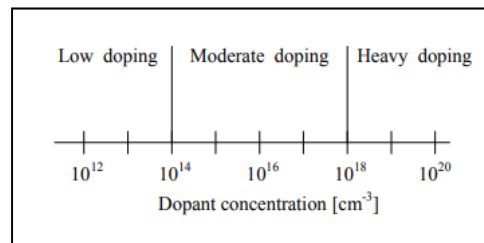
Figure 2.2 Doping ranges for Silicon
Taken from Zeman (2020)

2.4   Simulated subcell

Initially the subcell shown in Figure 2.1 is defined as the base of the simulation, in COMSOL using a 3D geometry. The parameters which are used to generate this cell are given in the Table 2.2. These parameters are chosen based on the model presented in (Fell *et al.*, 2014). As it is presented in this table, the base which is made of Silicon has 190 um thickness which is moderately doped. The Emitter and BSF are heavily doped, having a thickness of 1 um. To simplify the simulation, the third dimension has been chosen equal to the width of the base in order to create a cubic subcell.

Table 2.2 Subcell's parameters

	Width (um)	Thickness (um)	Doping
Base	790	190	Moderate
Emitter	490	1	Heavy
BSF	160	1	Heavy

The doping of the base, BSF and Emitter have an influence on the characteristics of the solar cell. To illustrate these effects, the model is simulated, for 10 different values of the doping for each region as shown in the Table 2.3. The minimum and maximum values are selected based on the doping ranges previously shown in Figure 2.2.

Table 2.3 Doping values

	Min (1/cm^3)	Max (1/cm^3)	Number of steps
Base	5.00E+15	5.00E+16	10
BSF	1.00E+18	1.00E+19	10
Emitter	1.00E+19	1.00E+20	10

2.4.1   Doping of base

The model is studied considering constant doping for the BSF and the Emitter, while the doping of the base varies from 5e15 per cm^3 to 5e16 per cm^3. The derived values of Voc, Jsc and efficiency are illustrated in Figure 2.3. Regarding the value of Voc, the increase in the doping of the base leads to rise in the open-circuit voltage by around 0.04 V. The changes of Voc versus doping of the base are semi-linear, with a positive slope. However, the influence of the doping reduces if the doping of the base is greater than 2.5e16 per cm^3. On the other hand, the value of Jsc sees a considerable reduction, from around 40.7 mA/cm^2 to 38.3 mA/cm^2

when the doping of the base increases. As for the performance of the cell, the efficiency rises considerably until reaching the peak of 17.7% when the doping is equal to 2e16 per cm³. Increasing the doping to values more than 2e16 per cm³, results in a reduction of the efficiency until around 17.4%.

In conclusion, the impact of modifying the doping of the base, influences the performances of the cell. The efficiency of the cells sees the stronger impact, this impact is stronger if the doping values of is less than 2e16 per cm³. With the current configuration, the best efficiency is reached when the doping of the base is equal to 2e16 per cm³.
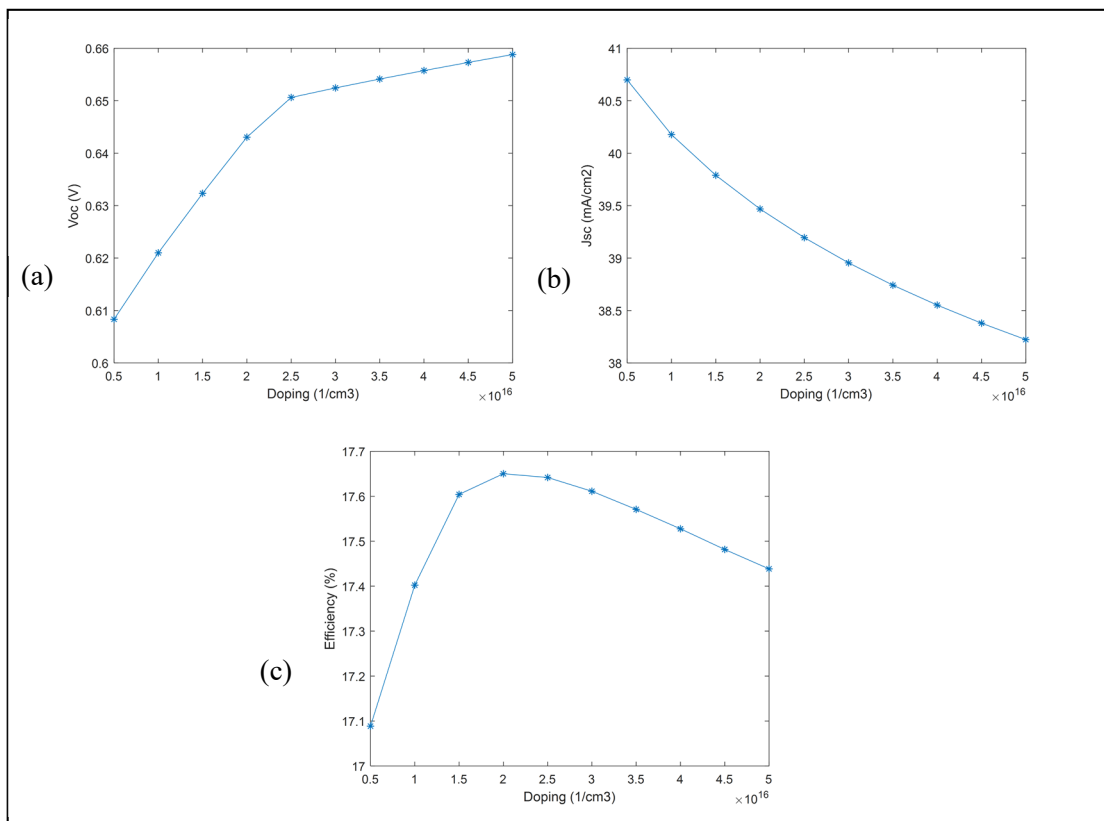
Figure 2.3 Effects of base's doping on the performance of the cell
(a) Voc (b) Jsc (c) efficiency

2.4.2   Doping of BSF

To study the impacts of the BSF's doping on the characteristics of the subcell, the doping of BSF is increased from 1e18 per cm^3 to 1e19 per cm^3, while the doping of the base and of the emitter remain constant. Figure 2.4 illustrates a minor increase of the value of Voc by increasing the value of the doping of the BSF. It increases from around 0.635 V up to 0.644 V along with the doping of the base. This impact is stronger on the value of Jsc as it increases of around 4 mA/cm^2, rising from 36.5 mA/cm^2 up to 40.5 mA/cm^2. These changes lead to increase in the efficiency from 16% when the doping of the BSF is equal to 1e18 per cm^3 up to 18% when the doping of the base equals to 1e19 per cm^3.

As a conclusion, the results of the simulations show that by increasing the doping of BSF from 1e18 1/cm^3 to 1e19 1/cm^3, results in an increase of the values of Voc, Jsc and of the efficiency.
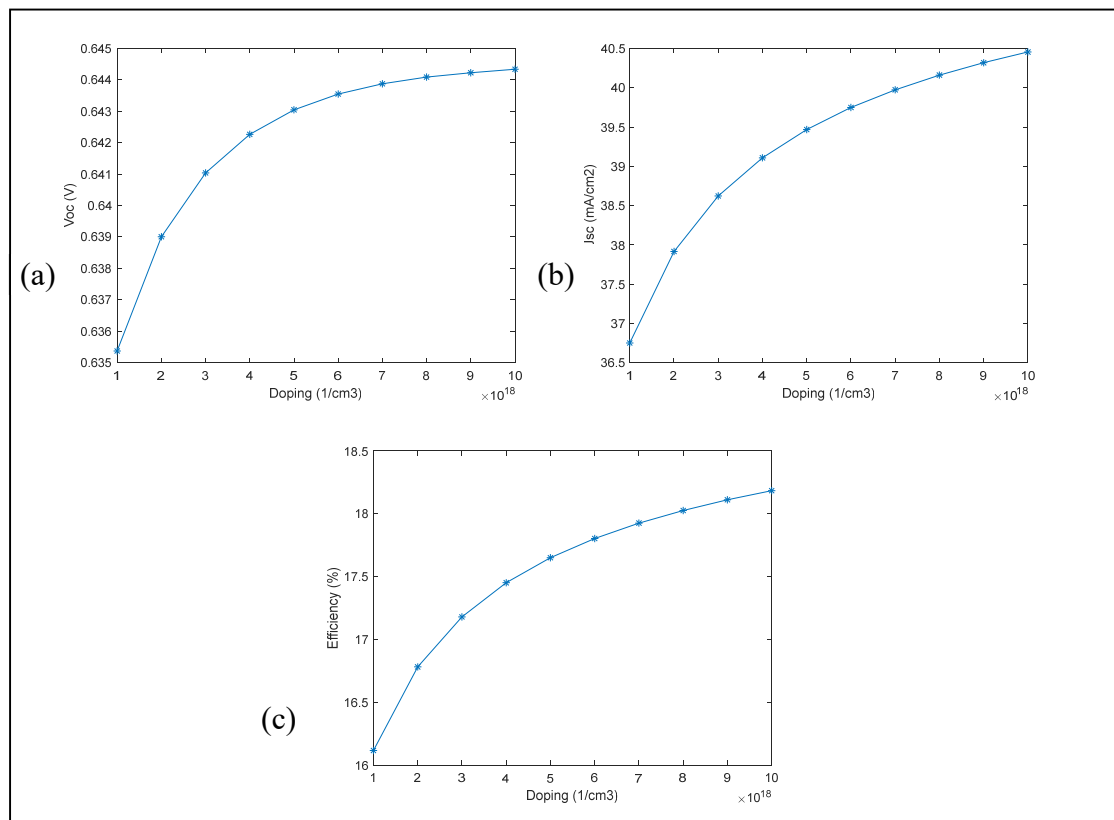
Figure 2.4 Effects of BSF's doping on the performance of the cell
(a) Voc (b) Jsc (c) efficiency

2.4.3   Doping of Emitter

To study the influence of the doping of the emitter on the performance of the cell, the doping of the base and BSF are fixed as constant values, while the Emitter's doping increases from 1e19 per cm^3 to 1e20 per cm^3. As shown in Figure 2.5, the value of Voc slightly decreases from 0.65 V to 0.63 V when increasing the doping of the emitter. On the other hand, the value of Jsc gradually increases from around 39.1 mA/cm^2 until 39.7 mA/cm^2 when increasing the doping of Emitter. Regarding the performance of the cell, increasing the doping of the Emitter, results in an increase of the efficiency until 17.65%, which happens when the doping of the emitter is equal to 5e19 per cm^3. If the Emitter's doping is higher than 5e19 per cm^3, then the efficiency drops moderately until reaching 17.54%.
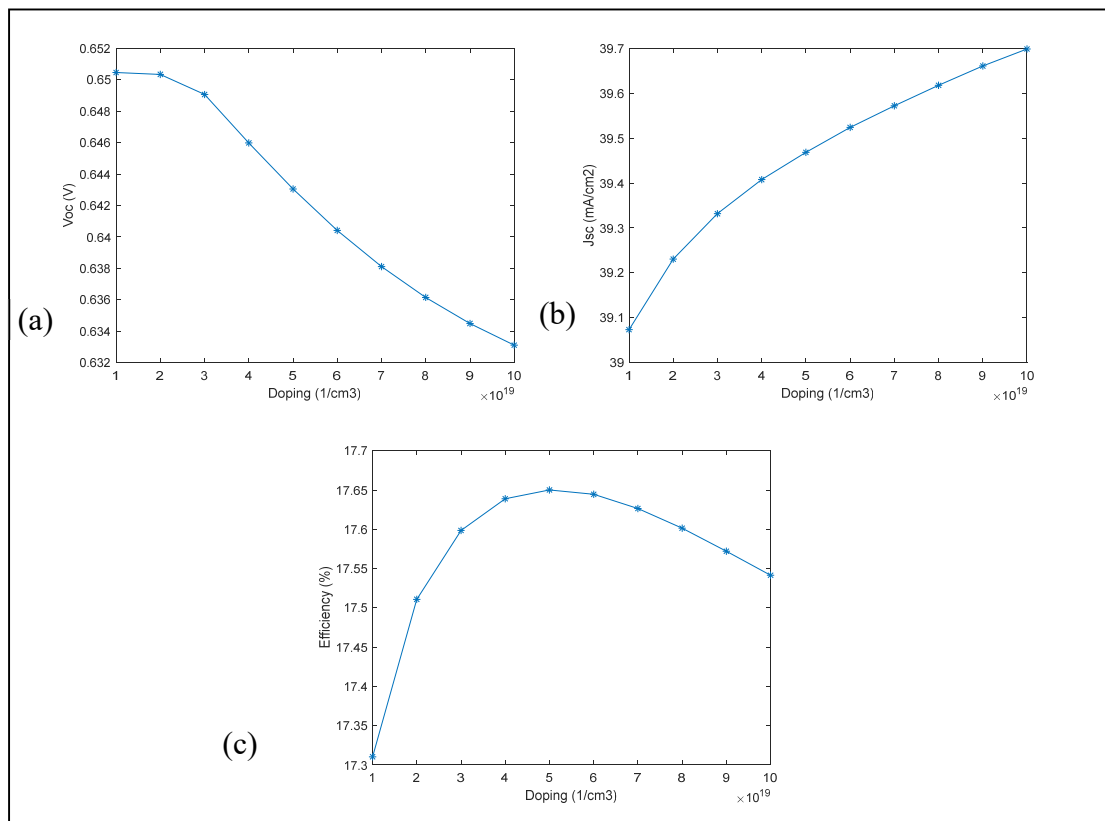
Figure 2.5 Effects of Emitter's doping on the performance of the cell
(a) Voc (b) Jsc (c) efficiency

In conclusion, the impact of modifying the doping of the Emitter, influences the performances of the cell. The efficiency of the cells sees the stronger impact, this impact is stronger if the doping values of is less than 4e19 per cm^3. With the current configuration, the best efficiency is reached when the doping of the base is equal to 4e19 per cm^3.

In general, changing the doping of the regions leads to negligible changes in the Voc. The changes in the Jsc are clearer as a function of doping. This leads to moderate changes in the efficiency while changing the doping of the regions.

Considering the effects of the doping, and the parameters used in previous studies and due to the fact that the fabrication process of the solar cells is confidential, the values of the doping of the simulated model have been chosen as 2e16 per cm^3 for the base, 5e18 per cm^3 for BSF and 5e19 per cm^3 for the Emitter.

2.5   Final model

To finalize the representing model and minimize the effects of the edges, the JV curve is studied for different number of subcells from 1 single subcell to a model including 10 by 10 subcells (Figure 2.6). Analyzing the JV curves shows that the model consists of a single block appears as an outlier due to the effects of the edges. This effect quickly disappears when using several subcells in an array.
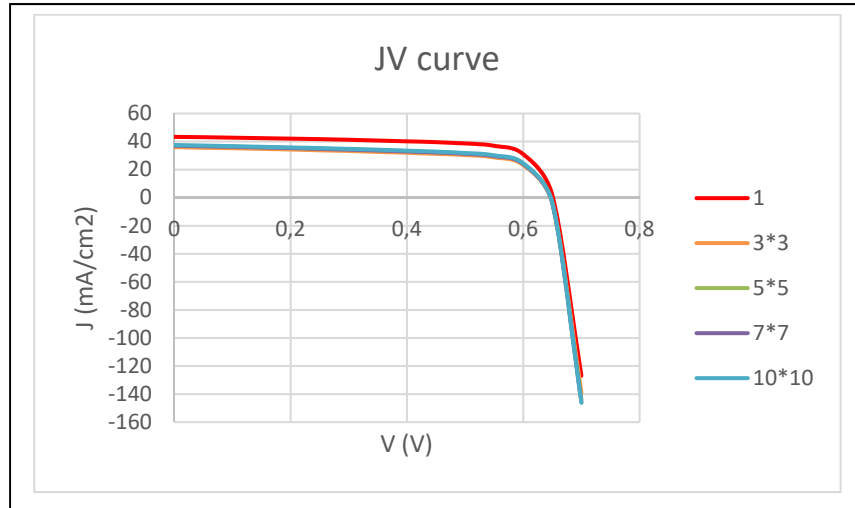
Figure 2.6 JV curves for different number of subcells

To provide a more precise analysis, the derived values of Voc, Jsc and efficiency for each case are plotted in Figure 2.7. It should be noted that increasing the number of subcells to 3*3 results in a decrease of these 3 parameters. Regarding the value of Voc, increasing the number of subcells from 1*1 to 3*3 results in a minor reduction of 0.01 V. Considering the value of Jsc, the 3*3 model shows around 9 mA/cm² reduction of the short-circuit current density when compared with the 1*1 model. Regarding the efficiency of the cell, the increase in number of blocks from 1*1 to 3*3 results in a considerable drop of around 5% in the efficiency of the cell.
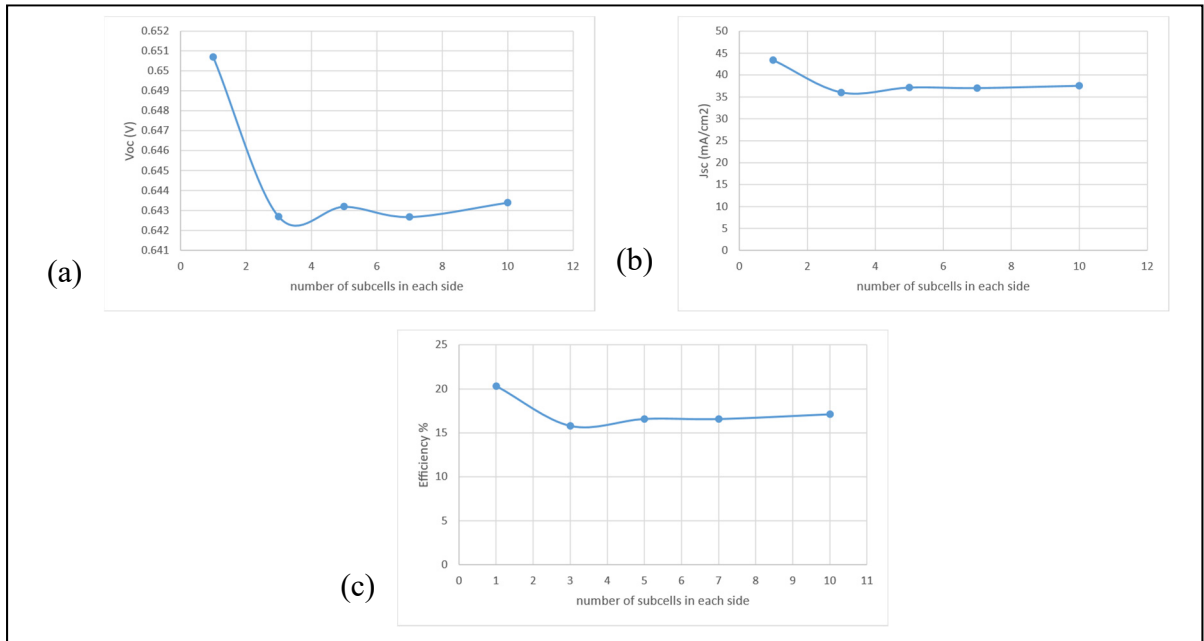
Figure 2.7 Effects of the number of subcells on the characteristics
(a) Voc (b) Jsc (c) efficiency

Regarding the models having from 3*3 up to 10*10 subcells, the parameters show almost the same saturated values. This effect occurs due to the removal of the influence of edges on the results of the simulation. To provide a compromise between the time needed to perform the simulation and the complexity of the model, a model containing 5*5 subcells is chosen as the final model. This model is shown Figure 2.8.
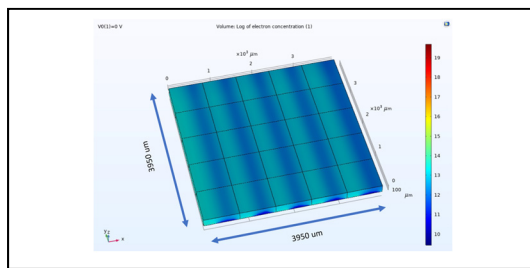
Figure 2.8 Final 5*5 model in COMSOL

2.5.1   Characteristics of the final model

Considering 1 sun illumination on the final 5*5 model, the JV-PV curves are shown in Figure 2.9. A simulation step of 0.05 V has been chosen. This step ensures a reasonable simulation

time while still providing accurate results to extract Jsc, Voc and Pmax. Analyzing this figure shows a short-circuit current density of around 37 mA/cm^2 and an open-circuit voltage of 0.64 V. The efficiency of the simulated model under an illumination of 1 sun is around 16.5%.
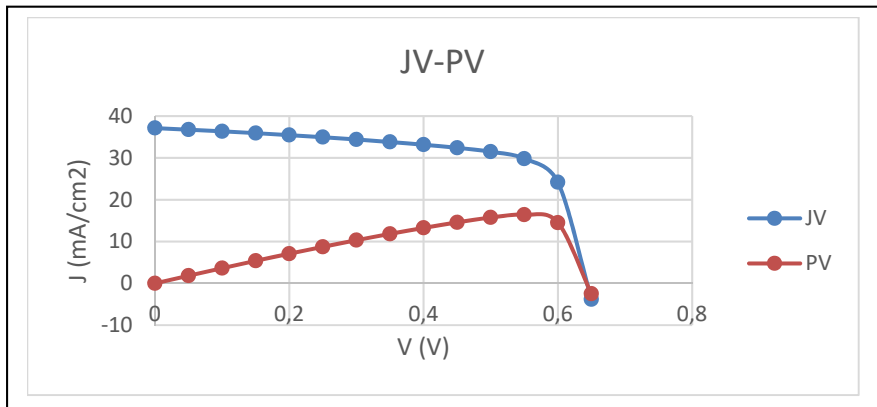
Figure 2.9 JV-PV curves for the final model

In order to validate the simulated model, the parameters extracted from the JV curve are compared with SunPower-Maxeon GENIII back-contact solar cell. As it is presented in Table 2.4, the simulated model is in accord with the actual solar cell's open-circuit voltage and short-circuit current by having negligible differences of about 0.06 V and 2.8 mA/cm^2 respectively. Considering the fill factor and efficiency, the simulated model shows lower values while staying in the normal ranges defined for solar cells. This occurs due to severe dependency of the fill factor and efficiency to the doping values and the dimensions of the doped area. As the exact values of doping and geometry of regions are confidential and not accessible, there is a difference between the efficiency of the simulated model and the actual solar cell. However, this does not have effects on the objective of this project as it is a comparison between the behavior of the simulated cell in normal condition and non-uniform illumination. Considering all, the simulated model can represent the reference model for further studies in this thesis.

Table 2.4 Comparison between simulated model and Maxeon
GEN III

	Simulated model	Maxeon GEN III
Voc (V)	0.64	0.7
Jsc (mA/cm^2)	37.14	39.9
Fill factor	68.9%	81%
Efficiency	16.5%	23%

2.6   Concentrated illumination

The changes in the light intensity affect the characteristics of the solar cell in different ways. As for the current, increase in the number of photons leads to rise in the generation carriers and so does the current. This linear ratio is shown by equation (2.1), in which X is the illumination intensity in sun, Isc is the short-circuit current under 1 sun illumination and I'sc stands for the new short-circuit current in case of concentrated illumination.

$$I'sc = X * Isc \tag{2.1}$$

Furthermore, the open-circuit voltage and the efficiency change logarithmically by increasing the light intensity, shown in equations (2.2) and (2.3) respectively.

$$V'oc = Voc + \frac{nkT}{q} \ln(X) \tag{2.2}$$

$$\eta' = \eta + \left(\frac{nkT}{q * Voc} * \ln(X) \right) \tag{2.3}$$

In these equations, k stands for Boltzmann's constant, T for temperature in kelvin, η for the diode ideality factor, and q is the electronic charge. V'oc and η' are the new values of open-circuit voltage and efficiency in concentrated illumination. Regarding the efficiency, both

output power and input power are having impacts on the performance of the cell and this relation is previously shown in equation (2.3). The power losses due to series resistance increases exponentially relatively to the concentration, this relation is shown in equation (2.4). In this equation, Rs stands for series resistance and Ploss stands for power loss.

$$\mathrm{Ploss} = \mathrm{X}^2 * \mathrm{Isc}^2 * \mathrm{Rs} \qquad\qquad (2.4)$$

The major increase in Ploss due to concentration leads to minor changes in the efficiency by increasing the concentration. Moreover, the efficiency has the limitation of the power losses due to the series resistance. Therefore, there is a theoretical limit regarding the maximum possible efficiency in high concentration solar cells.

In order to study the effects of the light intensity on the simulated model, the model is studied under different light intensity between 1 sun to 24 sun. The derived parameters are compared with the theory according to equations (2.1), (2.2) and (2.3) using Matlab.

As illustrated in Figure 2.10, the short-circuit current density shows great agreement with the theory, changing linearly when the light intensity increases from 1 sun to 24 sun. Regarding the value of Voc, the simulated model shows the same trend as the theory, with a negligible difference of 0.01 V between the simulation and theory when the light intensity is 24 sun. Analyzing the efficiency in different concentrated illumination shows having the same direction as the theory by having with a difference of less 0.6% when the illumination if equal to 24 sun. In general, the comparison between the results obtained from COMSOL simulation and theory verifies the good performance of the COMSOL model to represent the actual solar cell under concentrated light.
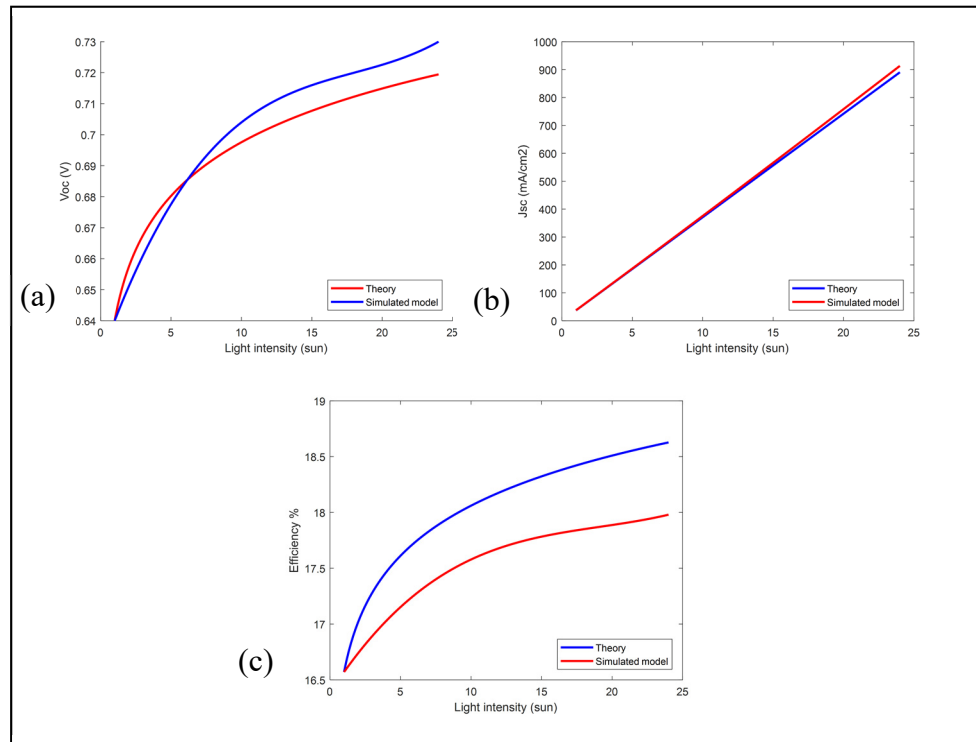
Figure 2.10 Comparison between cell's characteristics and the theory, in different light intensity (a) Voc (b) Jsc (c) efficiency

2.7 Effects of the temperature

To study the effects of the temperature on the efficiency of the cell, the modeled block is studied under 1 sun illumination. The temperature at which the simulations are performed varies from the standard temperature of 25 ˚C up to 65 ˚C. From the extracted IV curve, the efficiency for each temperature is calculated. The influence of the temperature on the efficiency of the solar cell is plotted and shown in Figure 2.11 . These results show a considerable drop in the efficiency as the efficiency is around 16.5% when the temperature is 25 ˚C, but only 13.8% when the temperature reaches 65 ˚C. This reduction in the efficiency due to increase of the temperature is in agreement with the literature. For the following simulations, in order to reduce the effect of the temperature on the simulation results, it has been determined to perform the simulations using a temperature of 25 ˚C.

32
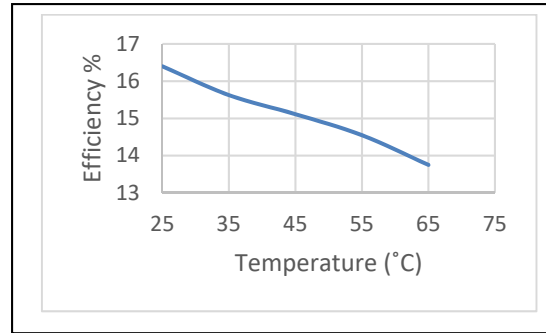
Figure 2.11 Effects of the temperature on
the efficiency, having 1 sun illumination

2.8 Non-uniform illumination

The Gaussian profile is considered as the main profile of non-uniform illumination as it occurs more often in concentrated solar cells using trough mirrors, which is the objective of this thesis. To study the effects of this non-uniform pattern, the model is studied in three different cases:

- When the non-uniformity occurs across the metal contacts.
- When the non-uniformity occurs along metal contacts.
- Combination of first and second cases (2D non-uniformity).

2.8.1 Non-uniform illumination across metal contacts:

Assuming the nonuniformity across the metal contacts (Figure 2.12) while having constant illumination along the contacts, and assuming the average of 1 sun illumination, different Gaussian profiles have been defined, shown in Figure 2.13. For all of the profiles, blocks 2 and 4 are considered as receiving constant illumination of 1 sun while the illumination of the central block and the edges change from zero to 3 sun, in order to achieve the average of 1 sun illumination on the whole model.

For the profiles 1 to 6, the central subcell is the most illuminated block which is happening more common in the experimental conditions. Profile 7 represents the uniform illumination of

1 sun on the whole model, and the reverse profiles 8, 9 and 10 present the condition with more illumination on the edges than the central block.
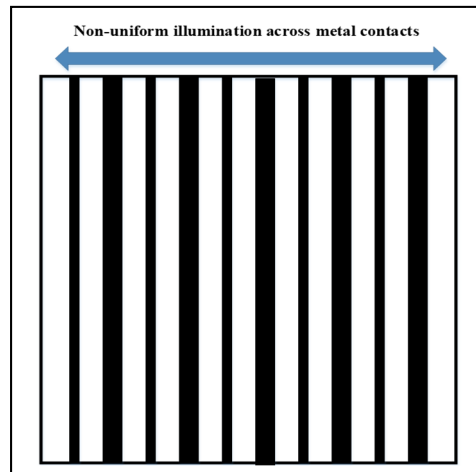
Figure 2.12 Non-uniformity across
metal contacts
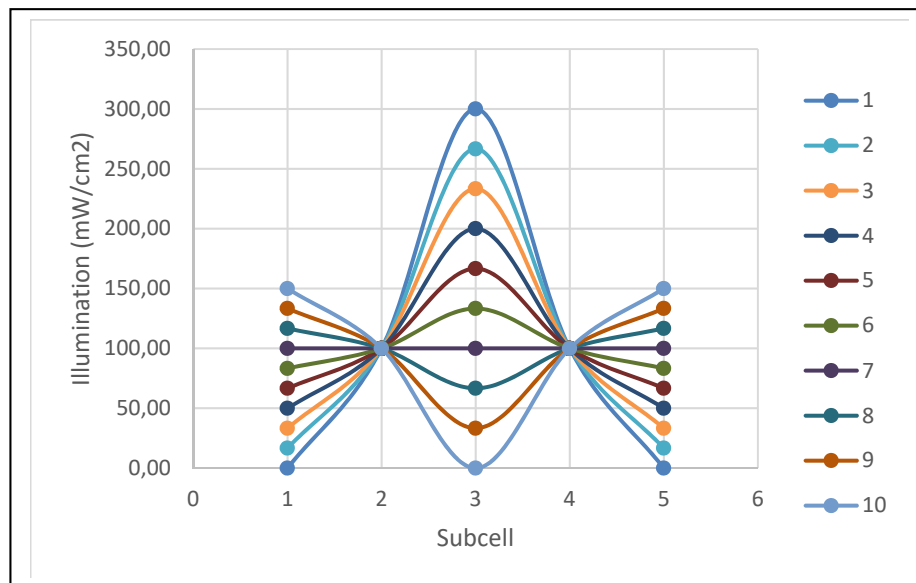
Figure 2.13 Illumination profiles across metal contacts,
having average of 1 sun

To get a better understanding of non-uniform illumination ratio, (Reis *et al.*, 2015) defines the non-uniformity factor (r), as the ration between the different of maximum and minimum illumination, and the average, shown in equation (2.5).

$$r = \frac{\text{Rmax} - \text{Rmin}}{\text{Ravg}} \tag{2.5}$$

In this equation, Rmax and Rmin stand for the maximum and minimum values of the light intensity, and the Ravg is the average of the illumination profile on the whole model. Considering this equation, the sharpest Gaussian pattern shows higher r values while in case of having a uniform pattern, the r-factor equals to zero. The calculated r-factors for each illumination profile is presented in Table 2.5. Analyzing the results shows the limitation of the r-factor as it cannot distinguish between the profiles with maximum illumination on the middle subcell and the profiles with higher illumination on the edges. This is illustrated in the case of the patterns 8,9 and 10 which have the same r-factor as the patterns 6,5 and 4. The reverse patterns are denoted using the * symbol.

Table 2.5 Calculated r-factor

Pattern	1	2	3	4	5	6	7	8*	9*	10*
r-factor	3	2.5	2	1.5	1	0.5	0	0.5	1	1.5

The effects of the non-uniformity (r-factor) on the efficiency for 1 sun, 12 sun (low concentration) and 300 sun (high concentration), has been studied and is shown in Figure 2.14. The efficiency in general demonstrates higher values for normal patterns rather than reverse profiles. Both 1 sun and 12 sun illumination show the same trend towards having non-uniform normal Gaussian profile. For these two cases, the efficiency of the cell increases along with the non-uniformity of the illumination along the model. The increase for 1 sun illumination due to non-uniformity is negligible around 0.05% while in the case of the 12 sun illumination profiles, the changes of the efficiency are more significant. As the increase of the non-

uniformity results in an augmentation of the efficiency from 17.69% for uniform illumination profile up to 17.81% for the sharpest Gaussian profile. Regarding the reverse profiles, the non-uniformity across the metal contacts does not have a significant effect on the efficiency of the simulated model and the efficiency stays around 16.5%. However, the reverse Gaussian profiles lead to minor decrease of the efficiency for the cases having average illumination of 12 sun. In general, in low concentration, the highest efficiency happens while having the sharpest Gaussian profile among normal patterns; however, among the reverse profiles, increasing the r-factor leads to minor decrease in the efficiency.

On the other hand, in high concentration as it is the case for 300 sun, the non-uniformity has more significant impact on the efficiency. Regarding the normal Gaussian profiles, the efficiency sees minor increase until reaching a peak of 17.15% while having non-uniformity factor of 1. The efficiency then drops by increasing the degree of non-uniformity. This occurs due to the saturation. Regarding the reverse profiles in high concentration, the efficiency drops considerably from around 17% to around 16% by increasing the non-uniformity. In general, the uniform illumination shows better results rather than non-uniform patterns in high concentration while the non-uniformity occurs across the metal contacts.
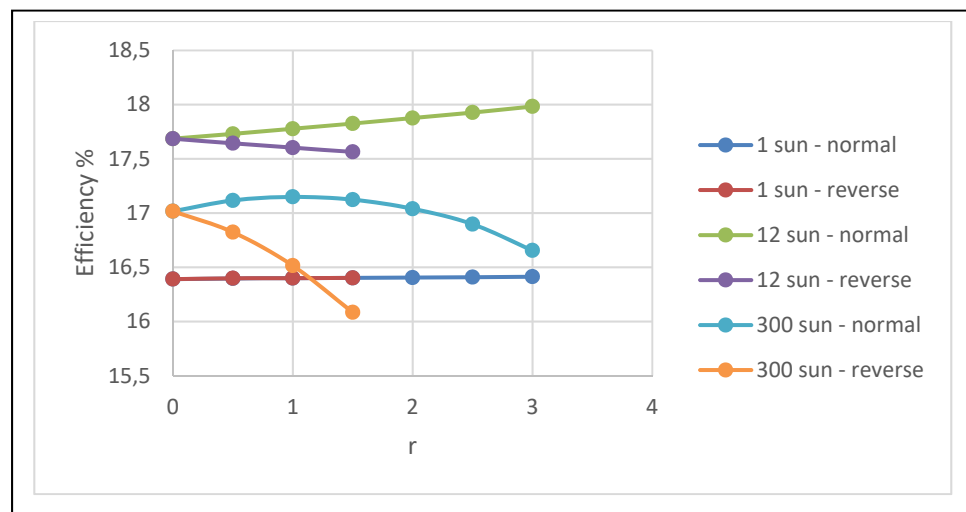
Figure 2.14 Efficiency changes versus r-factor, having the average illumination of 1 sun across metal contacts

2.8.2   Non-uniform illumination along the metal contacts

In this case, the non-uniform illumination happens along the metal contacts (Figure 2.15) while the illumination is considered as constant over the other dimension. The model is studied under the same illumination patterns as Figure 2.13 for 1 sun, 12 sun and 300 sun illumination.
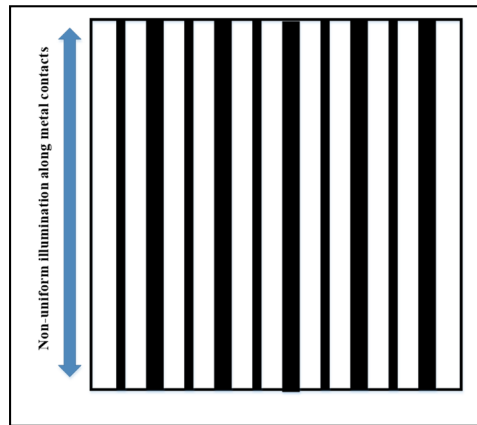
Figure 2.15 Non-uniformity along metal contacts

Analyzing the results derived from COMSOL (Figure 2.16) indicates that for 1 sun illumination, the non-uniform illumination which occurs along metal contacts does not have a significant impact on the efficiency. For this case, the efficiency sees negligible rise of 0.02% by increasing the non-uniformity factor from 0 to 3. Regarding 12 sun illumination, the rise of efficiency due to non-uniformity is more significant, as the efficiency is of 17.69% for uniform profile but of 17.78% for the sharpest normal Gaussian profile. The results obtained from reverse profiles show the same trend as the normal Gaussian profile. These reverse profiles have a negligible increase in the efficiency for 1 sun illumination and more considerable rise for 12 sun illumination due to non-uniformity.

Regarding 300 sun illumination and normal Gaussian profiles, the best efficiency happens when the illumination profile is uniform. This uniform illumination profile results in the efficiency of around 17%. The efficiency drops to until 16.2% when increasing the non-

uniformity factor to 3. As for the case of the reverse profiles, the non-uniformity across the metal contacts leads to a similar reduction of the efficiency as the correspondent normal profile.

In conclusion, the results of the simulation indicate that the non-uniform illumination along metal contacts have a minor positive effect on the efficiency in low concentration while in the case of high concentration due to the saturation, the cell under uniform illumination provides better performance.
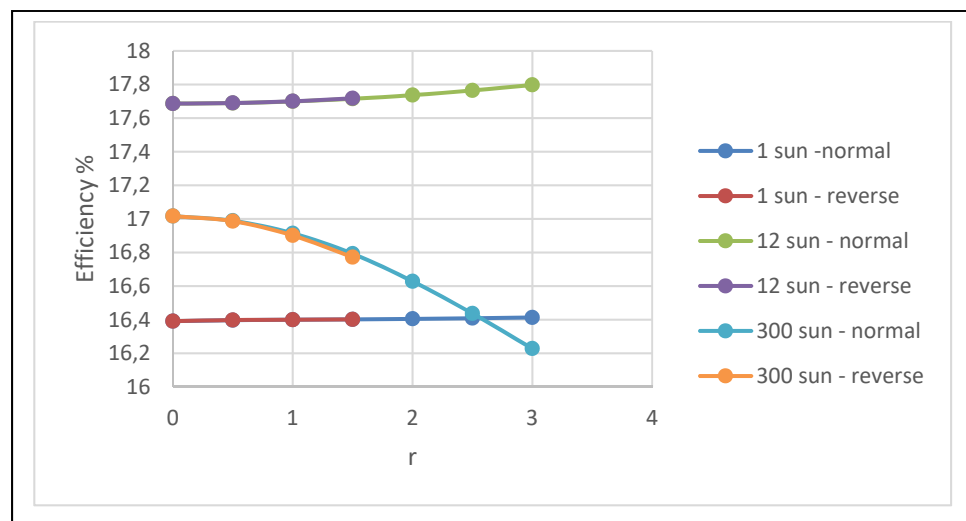
Figure 2.16 Efficiency trend while non-uniformity occurs along contacts

In order to study the influence of the non-uniform illumination location on the efficiency of the cell, the results obtained from non-uniformity across and along the metal contacts are analyzed and compared in Figure 2.17 for both normal and reverse profiles. Regarding the low concentration illumination, the non-uniformity which occurs along metal contacts has minor effects on the performance of the cell in both normal and reverse profiles. However, the impacts of the non-uniformity on the efficiency when it happens across the metal grid are more considerable. Moreover, the non-uniformity which occurs along the cell leads to minor improvements in the performance of the cell in both normal and reverse profiles; therefore, in

low concentration, the effects of non-uniform illumination along the metal contacts are negligible.
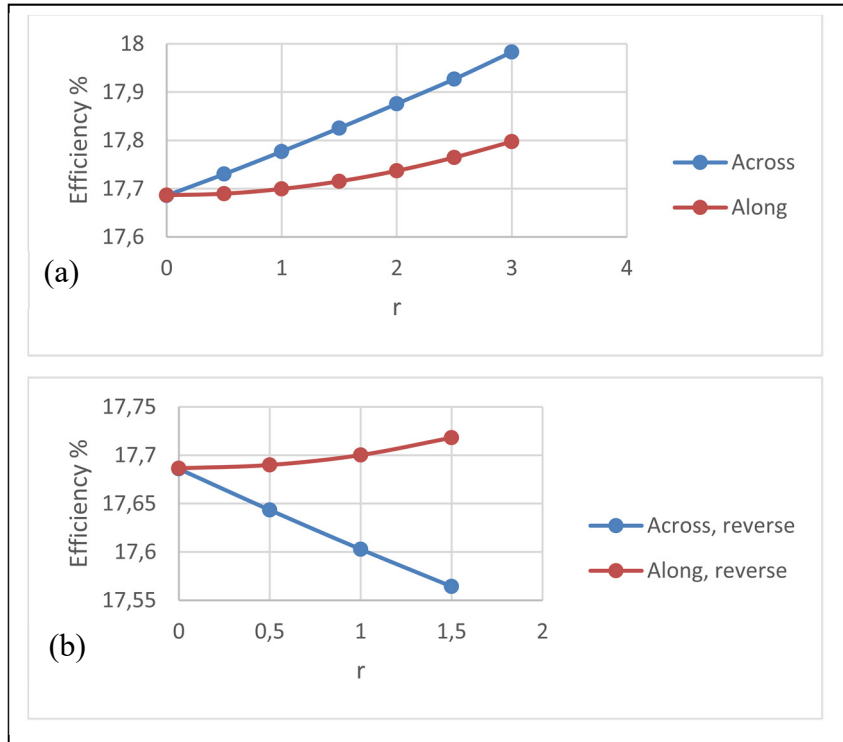
Figure 2.17 Comparison between location of non-uniformity over the cell in low concentration

Regarding high concentration, in normal Gaussian profiles, the impact of non-uniform illumination is more considerable while non-uniformity is located along the cell, by dropping the efficiency from 17% for uniform case to around 16.2%. However, for the case having non-uniformity across the cell, the impacts are minor. As for reverse patterns, although both cases see drops in the efficiency by increasing the r-factor, the decrease in the efficiency for the case having non-uniformity across the metal grid is more noticeable by dropping from 17% to around 16%. These impacts are shown in Figure 2.18.

In general, the comparison between the impacts of the location of non-uniform illumination on the performance of the cell shows that in low concentration, while having a cooling system to reduce the effects of temperature, the case having non-uniformity along the metal contacts is

less sensitive toward non-uniformity in both normal and reverse Gaussian profiles. On the other hand, in high concentration, the solar cell is more sensitive toward non-uniformity therefore based on the simulation results, for a concentrator that produces normal Gaussian illumination patterns, the solar cell should be located to receive the non-uniformity across the metal grids. If a cell is illuminated using a reverse Gaussian patterns, it is recommended to place the non-uniformity along the metal contacts, as in this case the cell is less sensitive to the non-uniformity.
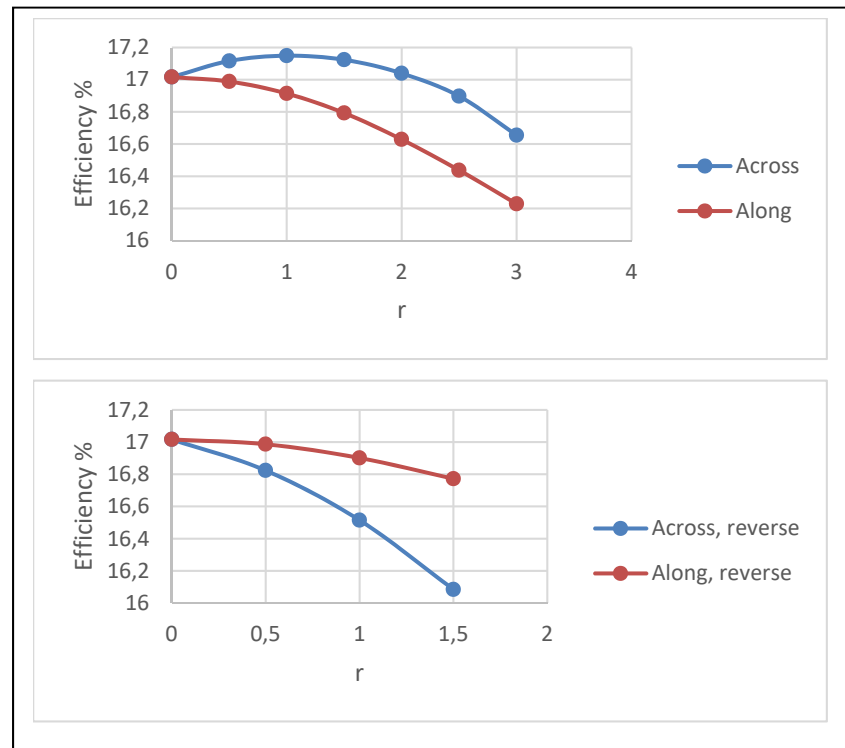
Figure 2.18 Comparison between location of non-uniformity over the cell in high concentration

2.8.3   Focus point illumination

In this case, which is the combination of the previous 2 cases, the illumination profile is considered as 2D non-uniformity as shown in Figure 2.19, having the most illuminated point

in the center of the 5*5 model, while the edges get less illumination. The blue blocks are considered to have constant illumination equal to the average illumination over the model while the central block and edges receive different illumination to generate different non-uniform illumination profile.
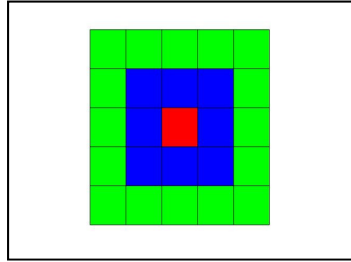
Figure 2.19 Focus point illumination

The model is studied having the 2D non-uniform illumination patterns while considering average illumination of 1 sun, 12 sun and 300 sun. In this section the reverse profiles are not considered as the normal Gaussian profiles are more common. As an illustration, the studied illumination profiles when the average illumination of equal to 1 sun are shown in Figure 2.20. For these profiles, the light intensity of the middle blocks, shown in blue in Figure 2.19, stays constant at 1 sun. While the illumination of the central block and of the blocks on the edge varies.
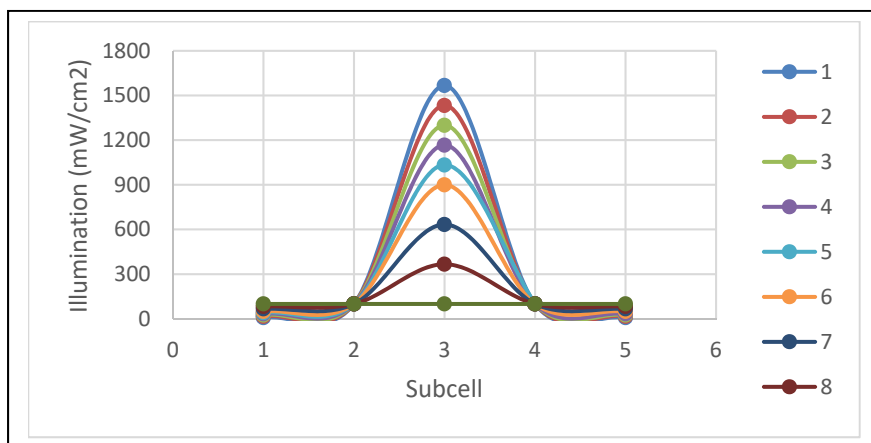
Figure 2.20 Illumination profiles of the focus point illumination, having average of 1 sun

The non-uniformity factor is calculated based on equation (2.5). For each profile, the efficiency is calculated and plotted in Figure 2.21. Analyzing the simulation results shows a minor increase in the efficiency by increasing the non-uniformity. When the illumination is equal to 12 sun, the efficiency slightly in decreases from 17.68% until the peak which happens 17.9%, this happens when the system has a severe non-uniformity factor of 14.17. Due to the appearance of saturation, the efficiency does not increase if the non-uniformity increases to 17. In case of high concentration, which is the case for 300 sun, the efficiency drops considerably by around 2% when the r-factor increases to 17. This occurs due to the saturation in high concentration.

In general, the results of the 2D non-uniform illumination over the simulated model shows minor improvements of the performance of the cell due to non-uniformity when the average illumination is low as it prevents the appearance of saturation. However, in high concentration, the non-uniformity leads to a severe drop in the efficiency of the simulated model.
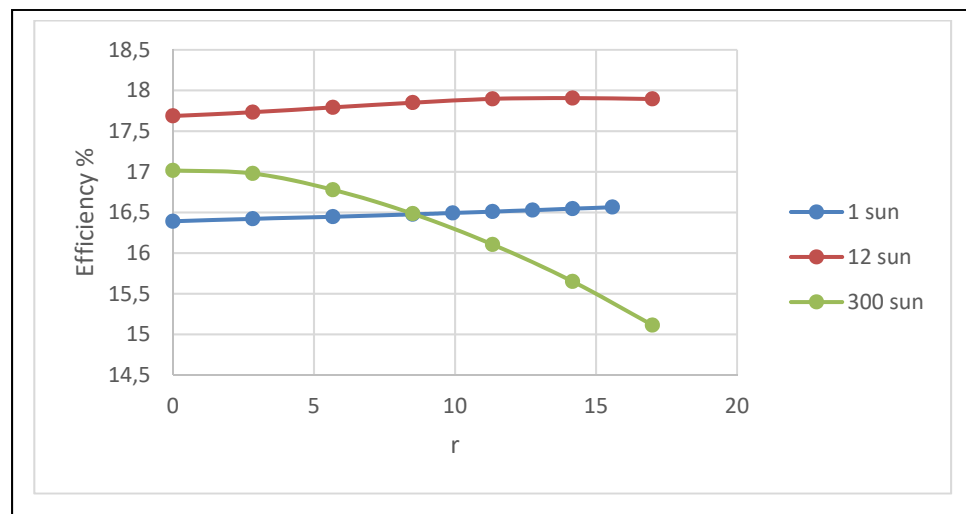
Figure 2.21 Efficiency changes versus r-factor in focus point illumination

2.9 Optimum illumination pattern

Based on the results obtained from the simulations for different Gaussian profiles, there are two cases to determine the optimum illumination pattern. For the case having low

concentration, as the saturation does not happen, the non-uniformity leads to better performance of the solar cell. In this case, the sharpest Gaussian profile, having the highest non-uniformity factor, leads to better efficiency of the cell. However, in high concentration, due to saturation, the uniform illumination pattern leads to better performance of the cell. For this case, by increasing the non-uniformity, the efficiency drops considerably.

For concentrator systems that the produced illumination is non-uniform in one direction, in case of keeping the solar cell at low temperature around 25, the case having non-uniformity along the contacts is less sensitive towards non-uniformity. This is coherent for both normal and reverse Gaussian profiles in low concentration and reverse profile in high concentration. Regarding the normal Gaussian profiles in high concentration, locating the solar cell to receive the non-uniformity across the metal contacts, leads to fewer impacts of non-uniform illumination on the performance of the cell. This is coherent with what has been presented in the literature.

2.10   Conclusion

In this chapter, a basic subcell block was proposed to model back-contact silicon solar cells. The effects of the doping of each region in the subcell were discussed as well. The behavior of the model was studied under different uniform light intensities which agreed with the theory. The suggested model was then studied under different Gaussian illumination profiles in 3 different cases: while the non-uniformity occurs across the contacts, along the contacts and combination of both cases.

It has been shown that if the intensity of the illumination is low then the non-uniformity of the illumination can lead to a small increase of the efficiency of the cell; however, this is only valid for low illumination. In the case of high illumination, the non-uniformity is detrimental to the performance of the cell as it decreases its efficiency.

CHAPTER 3

MEASUREMENTS

3.1 Introduction

In order to verify the results achieved by simulation experimentally, the characteristics of the sample solar cell is studied in the laboratory under different conditions. The solar cell is initially characterized under uniform illumination to derive the reference parameter values of the cell. A method to generate and measure the non-uniform concentrated illumination is proposed and the impact of such non-uniformity on the efficiency of the cell is studied.

The sample back-contact solar cell which is used in the experiments is the Sunpower Maxeon Gen III (12.5 cm*12.5 cm), which is cut in strips of 2.5 cm width. The datasheet of the reference solar cell is presented in ANNEX I.

This modified cell is shown in Figure 3.1. The copper bars are attached to present a positive and a negative electrode. This cell is used in Innovative solar power under low concentration, having parabolic trough. Due to the non-uniformity which occurs using parabolic trough, studying the impacts of the non-uniform illumination on the efficiency is of a great value.
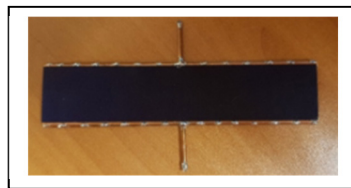
Figure 3.1 Sample solar
cell under study

ETS laboratory provides the Newport solar simulator, Model 91160-1000 (class AAA), which produces uniform 0.7 sun illumination, measured using light-meter (LI-250A) on an area of about 7 cm*7 cm. The light beam cannot cover the entire surface of the cell under study therefore, a method is proposed to have control on the illuminated area.

3.1.1   Setup for the illuminated area

To have a control on the illuminated area, a box made of PETG (Polyethylene Terephthalate Glycol-modified) is proposed to cover the cell. This box has been made using 3D printing. The top part of this box is a shield with different circle apertures. This material is chosen due to its high softening temperature around 85 ˚C, this ensures that the temperature changes due to concentration of light cannot affect the shape of the apertures. The top cover of the box slides so that different apertures can be used in the experiments. The apertures allow light to illuminate a particular area of the cell. The schematic of the box as well as the real box is shown in Figure 3.2. The smallest aperture has the diameter equals to 0.5 cm which illuminates an area equal to 0.2 cm², the diameter of apertures gradually increases with steps of 0.5 cm until the diameter of the aperture is of 2.5 cm.
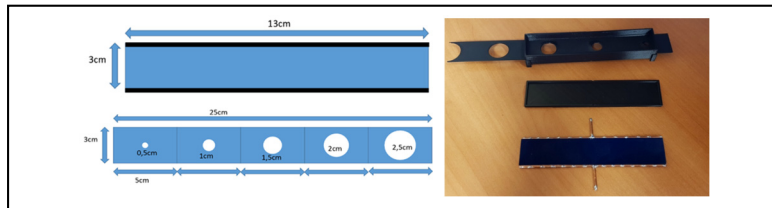
Figure 3.2 The schematic of the box used in the experiments

3.2   Reference values

To study the impacts of illuminated area's size on the efficiency of the cell, the sample solar cell is exposed to the light, having the largest possible illuminated area using a shield with an aperture that covers half of the cell as well as having different circle apertures to illuminate smaller areas of the cell. The temperature is monitored using thermocouple to ensure that measurements are taken at 25 ˚C. The Keithley 2400 source meter and its software interface allow the characterization of the solar cell. The setup is set to check 50 different points, and the related voltage and current are exported to an excel file. A Matlab code is used to plot the related JV curve and extract the open-circuit voltage, short-circuit current density, Maximum power point and related efficiency for each of the measurements results.

Moreover, these measurements have been repeated for the same apertures in the UQAM laboratory with the solar simulator model LSH-7320 (class ABA), which provides 1 sun uniform illumination, and the derived data is once again analyzed using Matlab. The extracted values for Voc, Jsc and efficiency are plotted versus different illuminated area and shown in Figure 3.3 for both 0.7 sun and 1 sun illumination.
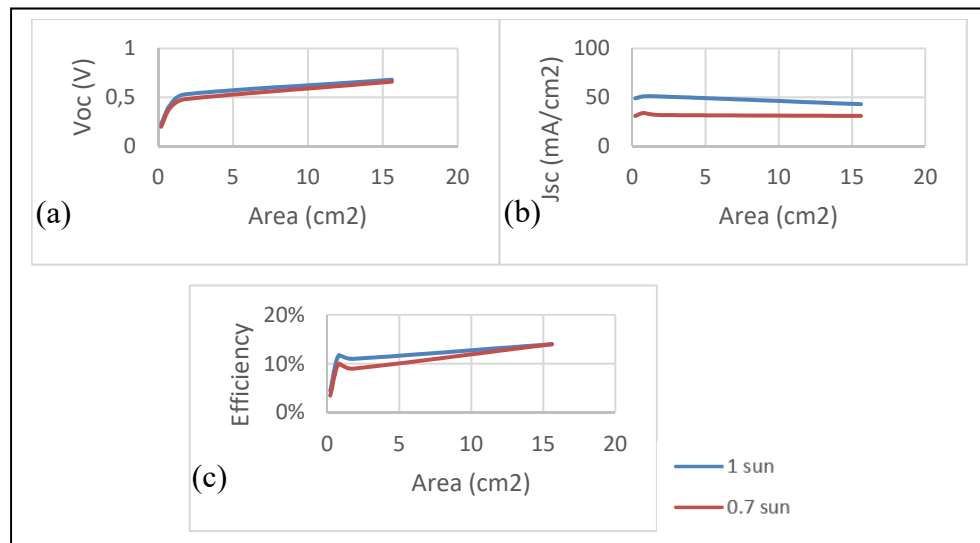
Figure 3.3 The (a) Voc, (b) Jsc and (c) efficiency of the sample solar cell
while the illuminated area changes, in 0.7 sun and 1 sun illumination

In 0.7 sun illumination, the open-circuit voltage decreases from 0.66 V for illuminated area is equal to 15.6 cm^2 to 0.2 V when the illuminated area decreases to 0.2 cm^2. The Voc follows the same trend in 1 sun illumination as well by decreasing considerably from 0.68 V to 0.23 V when the illuminated area decreases. The low open-circuit voltage while having small illuminated area happens due to the large shading effect. As an example, for the case having aperture of 0.2 cm^2, only 0.64% of the cell is illuminated which leads to low Voc. Regarding the short-circuit density, in 0.7 sun illumination by reducing the aperture's size the Jsc changes slightly from 32 mA/cm^2 to 31 mA/cm^2, reaching a peak of 34 mA/cm^2 when having illumination on an area equals to 0.79 cm^2. In 1 sun illumination, the Jsc has the same trend as 0.7 sun, being around 42 mA/ cm^2 when half of the cell is illuminated. As for the efficiency, the best efficiency achieves while having the largest illuminated area in both 1 sun and 0.7 sun

by having efficiency of around 14%. Decreasing the size of the apertures leads to drop in the efficiency, till 3.5% for 0.7 sun and 4.5% for 1 sun illumination. The low efficiency for small illuminated area happens due to the large shading over the cell. This is in good agreement with the literature as shown in (Al Mamun, Hasanuzzaman et Selvaraj, 2017).

Moreover, analyzing the results obtained for 0.7 sun and 1 sun illumination shows that all the three previously discussed parameters see minor rise by increasing the illumination from 0.7 sun to 1 sun. This is coherent with the theoretical performance of the solar cell.

The measurements results in both UQAM and ETS show the same trend toward changes in the illuminated area which verifies the proper performance of the solar simulator in ETS as well as the effects of the size of the illuminated area on the parameters of the solar cell. Thereafter, the results obtained for each illuminated area in 1 sun, is considered as reference for the further analysis in this chapter.

3.3 Effects of the temperature

The temperature has an effect on the performance of the solar cells therefore in the datasheets, the Standard Test Condition is defined as 25 ˚C for the temperature of the experiments. The temperature coefficients are defined as well for the voltage, current and power to illustrate the impact of the temperature on the parameters of the cell. For the cell under study, the temperature coefficients for voltage, current and power are defined as -1.74 mV/˚C, 2.9 mA/˚C and -0.29%/˚C in turns. These coefficients show the changes in the voltage, current, and power by each 1˚C increase in the temperature. By increasing the temperature, the current rises gradually while the voltage and power drop. Therefore, increasing the temperature leads to a drop in the efficiency of the solar cell.

Due to the concentration of the light, the temperature rises which affects the performance of the cell. In Innovative solar power, the water-cooling system is used to keep the temperature low while concentrating the light. This water-cooling system is composed of tubes, passing

around solar cells, that allows water to circulate and decrease the temperature. In ETS laboratory, a thermocouple is used to monitor the temperature during the experiments while the ambient temperature of the laboratory is fixed around 25 ˚C. The thermocouple is attached to the back surface of the solar cell. In (Al Mamun, Hasanuzzaman et Selvaraj, 2017) the relation between the back surface temperature and the solar cell's temperature for mono-crystalline Silicon solar cell is discussed. Therefore, the results obtained from the thermocouple are converted to achieve the solar cell's temperature based on the literature.

To illustrate the effects of the temperature on the characteristics of the solar cell, the cell is studied under 0.7 sun illumination at 25 and 40 ˚C, while half of the cell is illuminated. The results obtained for 40 ˚C are compared with the expected results from theory based on the temperature coefficients. As shown in Table 3.1 , increasing the temperature leads to rise in the short-circuit current density, from 31 mA/cm^2 when the temperature is 25 ˚C up to 32.2 mA/cm^2 when the temperature is equal to 40 ˚C. This measured Jsc is in good agreement with the expected impacts of temperature based on the datasheet by having 0.5 mA/cm^2 difference. As for the impacts of the temperature on the value of Voc, the measured open-circuit voltage at 40 ˚C is about 0.04 V less than the measured Voc at 25 ˚C, which is almost the same as calculated Voc based on temperature coefficient. Regarding the performance of the cell, the measured efficiency decreased from 14% down to 13.3% when the temperature is equal to 40 ˚C. This is 0.1% less than expected efficiency based on the datasheet, which in turns shows the accuracy of the experiments.

In general, the results show that the experimental results of the impacts of temperature on the parameters of the cell are in good agreement with the expected results based on datasheet, which once again verifies the accuracy of the measurements.

Table 3.1 Effects of temperature on the efficiency

Temperature	Voc (V)	Jsc (mA/cm2)	Efficiency
25 ˚C	0.66	31	14%
40 ˚C (measured)	0.62	32.2	13.3%
40 ˚C (theory)	0.63	33.7	13.4%

3.4 Concentrated illumination

Considering the available equipment in the laboratory, a Thorlabs optical lens is chosen to concentrate the light which is produced by the solar simulator. This lens concentrates the light at the focal point, which results in a Gaussian illumination profile. The lens is fixed at a specific height, using a lens holder to reach maximum illumination around 11 sun. The resulted light beam illuminates a small area around 2.5 cm by 2.5 cm, which justifies the idea of using the box having small apertures. In order to characterize the solar cell under this non-uniform illumination, the exact input power produced by the solar simulator as well as the non-uniform pattern should be measured.

3.4.1 Measuring intensity

Photodiode Thorlabs-DET10A allows measuring the pattern of the non-uniform illumination by converting the light into an electrical current. The photodiode is connected to an oscilloscope, with a resistance of 50 Ω to give the output voltage (Vph). To calibrate the photodiode and calculate the conversion factor, the output of the photodiode is compared with LI-250A light-meter, for different uniform light intensity. The conversion factor is shown in equation (3.1) which converts the output voltage of the photodiode in mV to the light intensity W/m^2.

$$\text{Light intensity} \left(\frac{W}{m^2}\right) = \text{Vph (mv)} * 60.87 \tag{3.1}$$

To measure the exact pattern of the non-uniform illumination while the lens is present, the illuminated area is divided into a grid. The area covered by the grid is chosen to contain different light intensities to ensure having a great range of non-uniformity. The light intensity is initially measured along the grid, using 2 MicroPositioners to ensure taking steps of 0.25 mm. The measured values are then converted to light intensity, using equation (3.1). The obtained illumination grid for an area equals to 7 mm*7 mm is shown in Figure 3.4 (a). Considering the time spent to achieve a small grid as well as the variation of the intensity

between grid's cells, the steps of 1 mm are selected to define the illumination pattern. The 2 cm by 2 cm grid is measured having steps equal to 1 mm this is illustrated in Figure 3.4 (b). The minimum illumination on this grid is around 0.06 sun on the edges while the maximum illumination is about 11 sun which occurs a few millimeters above the center of the grid. The average illumination over this grid is around 4 sun, and the r-factor based on equation (2.5) is around 2.7, which denotes severe non-uniformity along the grid.

(a)   (b)
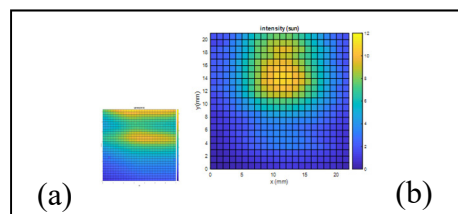
Figure 3.4 Light intensity grid with
steps of (a) 0.25mm (b) 1 mm

In order to study the effects of non-uniformity and in particular the r-factor on the efficiency, 4 points are selected on the grid. These points are to be placed as the center of the box's aperture, this is shown in Figure 3.5 along with the schematic of the box placed on the measured grid. As for the points 1, 2 and 3, the apertures having radius of 0.25 cm and 0.5 cm are selected as the case studies. The point number 4 is chosen on the center of the grid which allows to use a bigger aperture having radius of 0.75 cm to illuminate the solar cell. These points are selected to ensure having different illumination and non-uniformity factors, based on the measured grid.
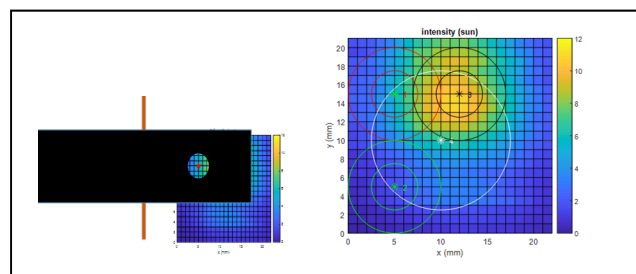
Figure 3.5 Selected illuminated area

The analysis of the illumination patterns over each location for the aperture is shown in Table 3.2. For each case, the maximum, minimum, the average illumination, and the r-factor is calculated based on the illumination grid. Analyzing the results shows that the chosen areas are having non-uniformity degrees from the least non-uniform case by having r-factor equals to 0.28 for case 5 to the most non-uniform case having the r-factor equals to 2.65 for case number 4. Regarding the average illumination, the most illuminated cases are happening for cases 5 and 6 which are located at the point 3 in the illumination grid, by having the average illumination around 9.6 sun and 8.6 sun respectively. The less illuminated area is happening around point 2 for the cases 3 and 4 by having almost 2 sun average of illumination. In general, the case having smaller illuminated area has lower r-factor than the case with a larger area for each of the first, second and third points. As for case number 7 which has the largest area, the average illumination is around 6 sun, covering from 1 sun to 11 sun illumination, which leads to r-factor equals to 1.6.

Table 3.2 The calculated r-factor of the selected case studies

Case	Point	Area (cm2)	Max (sun)	Min (sun)	Average (sun)	r-factor
1	1	0.2	8.2	3.4	5.8	0.83
2	1	0.79	10.17	2	5.63	1.46
3	2	0.2	2.98	1.2	1.99	0.89
4	2	0.79	5.66	0.36	2	2.65
5	3	0.2	10.77	8.1	9.64	0.28
6	3	0.79	10.77	5.66	8.1	0.64
7	4	1.76	10.77	1.5	5.79	1.6

3.4.2   Solar cell under non-uniform illumination

In order to study the influence of non-homogeneous illumination on the characteristics of the solar cell, the sample solar cell is placed inside the box, having different apertures and exposed to the light while the center of the aperture is located on the points 1 to 4. For each experiment, the extracted voltage and current are analyzed in Matlab to obtain the JV curve and extract the values of Voc, Jsc, and Pmax. The experiments are done for each point from 1 to 4, and this

cycle is repeated 5 times, to decrease the errors happening due to the misalignment of the box. As an illustration, the JV-curves obtained for case 7 are presented in Figure 3. 1. Case 7 is the case in which the largest aperture is used, the use of such aperture results in an average illumination of 5.79 sun. The results show minor errors in the experiments which in turns verifies the accuracy and repeatability of the measurements. This figure shows short-circuit current density of around 200 mA/cm^2 and open-circuit voltage of about 0.64 V for all the 5 experiments while there are negligible variations between curves.
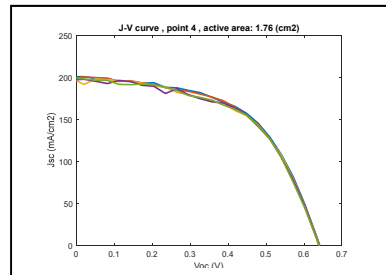
Figure 3. 1 Repeated JV curves for case 7

In general, the results of the repeated measurements for all the cases which have been presented in Table 3.2 show negligible errors in the parameters which verifies the accuracy and repeatability of the experimental method. Considering this, the average values of the experiments are chosen as the parameters of the cell for each setup.

The temperature is monitored using the thermocouple discussed in section 3.3. For the cases 1 to 5, the temperature stays around 25 ˚C when the measurements are being done. For the cases 5 and 6, due to the high average illumination of 9.64 sun and 8.1 sun, the temperature rises quickly during the experiments. Regarding case 7 which is the case where the illuminated area is of 1.76 cm^2, the total input power is high due to the large aperture area, which causes a quick rise in the temperature. As discussed in section 3.3, an increase in the temperature results in a reduction of the performances of the solar cell therefore in the next sections, the effects of the temperature for these three cases should be taken into account.

To study the behavior of the solar cell under different illumination, the average values of measured Voc, Jsc and efficiency of the cases 1 to 6 are plotted versus average illumination,

shown in Figure 3.6. Due to the experimental setup, it is not possible to get the same non-uniformity factor for different measurements therefore in this section, the r-factor is not taken into account and the results are plotted using the average illumination along the illuminated area.
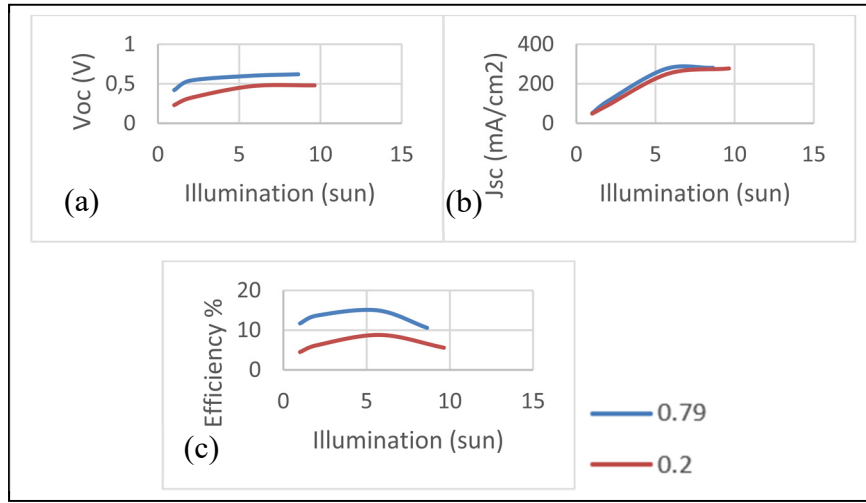
Figure 3.6 The effects of illumination on the
(a) Voc (b) Jsc and (c) Efficiency

For both illuminated area of 0.2 cm^2 and 0.79 cm^2, the open-circuit voltage rises quickly when the light intensity is lower than 6 sun. The Voc then stabilizes around 0.6 V and 0.5 V for the illuminated areas of 0.2 cm^2 and 0.79 cm^2 respectively, light intensity increases above 6 sun. Regarding short-circuit current density, both curves for apertures 0.2 cm^2 and 0.79 cm^2 show good agreement, increasing semi-linear until the illumination reaches 6 sun. The curves become flat if the light intensity is greater than 6 sun which shows reaching saturation when the illuminated area is relatively small (0.2 cm^2 and 0.79 cm^2). As for the performance of the cell, the efficiency reaches the peak around 6 sun illumination for both apertures. Before the occurrence of the saturation, the efficiency rises along with the increase of the light intensity. After reaching the saturation around 6 sun, the efficiency decreases along with the increase of the light intensity. The best performance of the cell happens for case number 2, having aperture size of 0.79 cm^2, when the efficiency equals to 15%, and average illumination of 5.6 sun, while

the less efficient case happens for case number 3, having 0.2 cm^2 illuminated area by having 6% efficiency under average illumination of 1.99 sun.

In general, both aperture sizes of 0.2 cm^2 and 0.79 cm^2 have the same trend towards increasing the average illumination. However, the values of Voc and efficiency for the cases having illuminated area of 0.79 cm^2 are higher than the cases having the same average illumination but smaller aperture of 0.2 cm^2. On the other hand, the Jsc for the cases having 0.2 cm^2 and 0.79 cm^2 illuminated area are having almost the same values which is due to the fact that the area is considered is relatively small.

Due to the available equipment and setup limitations, it is not possible to get the desired uniform concentrated illumination, having the light intensity equal to the average illumination over the cell in the cases presented in Table 3.2. Therefore, in order to study the impacts of non-uniform illumination on the characteristics of the cell, the results obtained from measurements should be compared with the theoretical results of uniform illumination, having the same average light intensity, illuminated area and temperature. To achieve this, the parameters extracted from measurements under 1 sun illumination in section 3.2 are used as the reference parameters, and they are presented in Table 3.3. This table shows the vales of Voc, Jsc and efficiency for different illuminated area of 0.2 cm^2, 0.79 cm^2 and 1.76 cm^2 in 1 sun uniform illumination and 25 ˚C.

Table 3.3 Reference parameters for different apertures, in 1 sun illumination

	Aperture 1	Aperture 2	Aperture 3
Area (cm^2)	0.2	0.79	1.76
Voc (V)	0.23	0.42	0.53
Jsc (mA/ cm^2)	49	51	51
Efficiency %	4.5	11.7	11

To calculate the Voc, Jsc and efficiency under a concentrated uniform illumination, the values measured under a 1 sun illumination for each aperture size are used along with the formulas previously discussed in section 2.6 in Matlab. The concentration ratio is selected based on the average illumination of each case, these were shown in Table 3.2. This, results in new values for Voc, Jsc and efficiency, considering uniform concentrated illumination.

Table 3.4 shows these new values for Voc, Jsc and efficiency, based on the average illumination over the cell and are identified using *. For these cases, the r-factor equals to zero as the calculation are done assuming uniform illumination. As it is mentioned in section 2.6, Voc and efficiency change logarithmically while the Jsc rises linearly by having greater values of illumination as shown in this table. It should be noted that the impacts of temperature are not considered in this table as the temperature was controlled to be 25 ˚C.

Table 3.4 Expected parameters for each case, based on reference values and theory

Case	Average illumination (sun)	V*oc (V)	J*sc (mA/ cm^2)	Efficiency* %
1*	5.8	0.28	284	5.4
2*	5.63	0.46	285	12.9
3*	1.99	0.25	97.5	4.8
4*	2	0.44	101	12.2
5*	9.64	0.29	472	5.6
6*	8.1	0.47	413	13.1
7*	5.79	0.57	292	11.9

It is necessary to take into account the influence the temperature on the calculated efficiency of each case. To achieve this, the temperature coefficients discussed in section 3.3 are used to compute the expected parameters of under concentrated uniform illumination at the temperature at which the measurements are performed. For each case, the efficiency is plotted considering the average illumination as shown in Table 3.4, for a standard temperature of 25 ˚C and the measured efficiency in the laboratory at specific temperature. As it is mentioned in the section 3.4.2, the temperature rises quickly for cases 5, 6 and 7 rather than other cases therefore the decrease in the efficiency due to temperature is more significant for these cases as shown in Figure 3.7.

For the cases 1, 2, 3 and 4 which are the cases receiving a light intensity less than 6 sun, the changes in the temperature during the measurements are negligible. Therefore, the effects of the temperature coefficients on the characteristics of the solar cell are minor. As for the cases 5 and 6 which are the cases receiving high average illumination of 9.64 sun and 8.1 sun respectively, the temperature rises quickly to around 55 ˚C during the experiments. This leads to a considerable drop of 0.5% and 1.1% in the efficiency of the solar cell in cases 5 and 6 respectively. The temperature of the Case 7 is the third highest temperature, with a temperature of about 50 ˚C. This is due to the large aperture which is used in this case (1.76 cm^2) and the relatively high concentration. For this case, the rise in the temperature leads to a reduction of around 0.86% in the efficiency.

Cases 1 and 2 are receiving relatively moderate average illumination. Therefore, the temperature does not increase quickly during the experiments. For these cases, slight changes in the temperature leads to a minor decrease of around 0.1% in the efficiency.

For cases 3 and 4 which are the cases having the lowest average illumination of around 2 sun, the temperature stays around 25 ˚C during the measurements; therefore they are not visible in the figure.
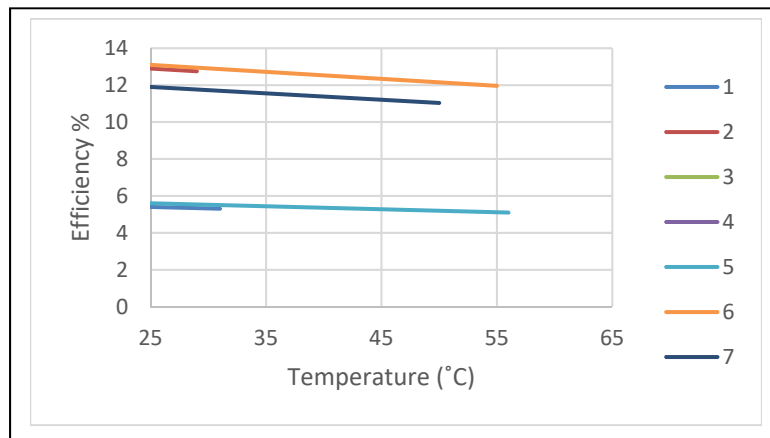
Figure 3.7 Effects of the temperature on the efficiency
for each case

To study the impacts of non-uniform illumination on the efficiency of the solar cell, the calculated efficiency giving consideration to the temperature's effect, light intensity and the illuminated area is compared with the results extracted from the measurements under non-uniform illumination and is shown in Figure 3.8. In this figure, the r-factor equals to zero presents the uniform case, having the same illumination as the average illumination for each case.

Analyzing the figure shows increase in the efficiency for all the cases except cases 5 and 6 versus non-uniformity factor, which are the cases receiving the highest average illumination and are located around point 3 on the illumination grid (Figure 3.5).
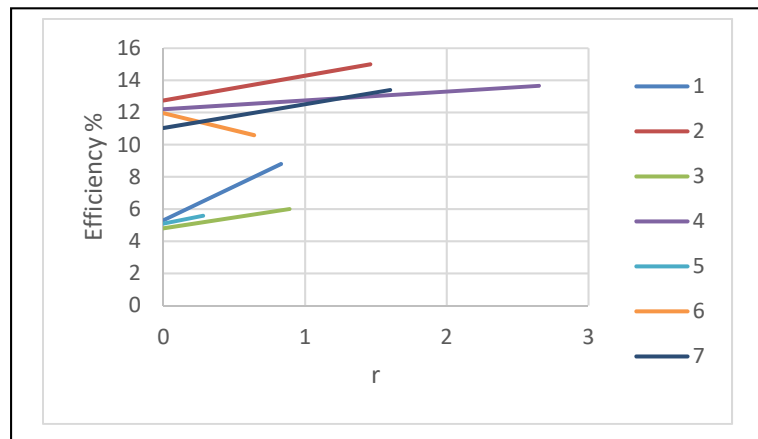
Figure 3.8 Effects of non-uniform illumination
on the efficiency

Among the cases which are having better performance due to the non-uniformity, cases 1, 2 and 7 are having higher positive slopes which validates the effectiveness of non-uniformity on the improvement of the efficiency while the average illumination is around 6 sun. On the other hand, cases 3 and 4 see rise in the efficiency as well while having a lower positive slope. These two cases are located around point 2 on the illumination grid and receive around 2 sun average illumination.

Regarding the cases 5 and 6, the cell receives high illumination average of 9.6 sun and 8.1 sun respectively. For these two cases, highly concentrated light illuminates small areas of 0.2 cm^2 and 0.79 cm^2. The produced generation carriers see saturation due to the small illuminated area which in turns leads to decrease in the efficiency. For these two cases, due to the saturation, the non-uniformity cannot lead to the rise in the efficiency, therefore the best performance of the cell in these cases happens while having uniform illumination. This is shown in Figure 3.8 for cases 5 and 6 with negative slope towards increase in the non-uniformity factor.

In general, the comparison between the efficiency in uniform and non-uniform illumination shows two different trends. If the saturation is not reached which is valid for cases 1, 2, 3, 4, and 7, the non-uniform illumination can lead to better performance of the cell. These cases are

receiving light intensities less than 6 sun. On the other hand, if the saturation happens as it is the case for the highly illuminated cases 5 and 6, the efficiency of the solar cell while having uniform illumination is greater than the efficiency measured for non-uniform illumination.

3.5 Optimization of the efficiency

There are several parameters that have impacts on the efficiency of the solar cell such as the average illumination, temperature and illumination pattern; therefore, to improve the performance of the cell, these parameters need to be optimized.

Based on the results obtained from the measurements of the solar cell under study, the temperature has negative effects on the performance of the solar cell. Therefore, in order to have the optimized performance of the cell, a cooling system should be used to ensure keeping the temperature around 25 ˚C.

Considering the average illumination, based on the theory the efficiency changes logarithmically by increasing the light intensity while in the reality, due to the saturation, the efficiency changes logarithmically until reaching a peak, then drops slightly. Due to the severe shading over the cell under study, the saturation happens while having around 6 sun average illumination during the experiments. Therefore, for the cell under study while having a small illuminated area, the best efficiency happens while the average illumination equals to 6 sun.

Regarding the illumination pattern, the experimental results show two different scenarios. In the first scenario, the average illumination is low therefore the saturation does not happen. In this case, non-uniformity leads to better performance of the cell. On the other hand, when the average illumination is high enough that the saturation happens, the uniform illumination profile shows better efficiency.

In general, the results show that in case of having optimal cooling systems to reduce the effects of temperature, in low concentration there is no need to invest in generating perfect uniform

illumination pattern as the non-uniformity leads to better performance of the cell. On the other hand, for higher concentration when the saturation happens, generating uniform illumination is of a great value as the non-uniformity leads to reduction in the efficiency.

3.6   Conclusion

In this chapter, a method to characterize the solar cell under non-uniform illumination was presented. This method consists of characterizing the sample solar cell under uniform 0.7 sun and 1 sun illumination. The light beam produced by solar simulator was then concentrated using a lens to achieve non-uniform concentrated illumination. The temperature was monitored to reduce the effect of temperature on the parameters of the cell. The parameters obtained from experiments for different light intensities and non-uniformity factors were compared with the theory, using Matlab.

The results showed improvements in the performance of the cell by having non-uniform illumination for cases having lower average illumination. The best performance was achieved having around 6 sun average illumination. Due to the small illuminated area, the saturation occurred for cases having average illumination more than 6 sun, which resulted in lower efficiency.

Considering all, the results obtained in experimental works showed that in lower average illumination, the non-uniformity can lead to rise in the efficiency in case that the temperature is in control. This verifies the results obtained from simulations in simulation chapter.

CHAPTER 4

VALIDATION

4.1   Introduction

In order to validate the accuracy of the simulated model in predicting the behavior of the cell, the results obtained from the simulation and measurements are compared and analyzed in this chapter. To have a clearer perspective, the results are compared in three different aspects:

- The effects of the light intensity on the efficiency
- The impacts of the temperature on the performance of the cell
- The impacts of the non-uniform illumination on the efficiency

In all these analyzes, the normalized efficiency is calculated for both simulation and measurements to allow a more straightforward comparison.

4.2   Effects of concentrated illumination

In CHAPTER 2, a COMSOL model of the back-contact solar cell is presented and the behavior in different light intensities is studied and compared with the theory. In order to validate it experimentally, the results obtained from COMSOL are compared with the experimental results as well as the theory and shown in Figure 4.1.
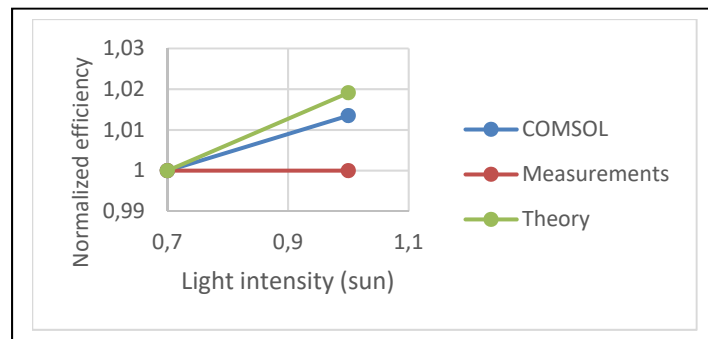
Figure 4.1 Effects of light intensity on the efficiency in COMSOL, experiments and theory

The results shown in this figure are the normalized efficiency obtained considering 0.7 sun and 1 sun illumination. Regarding the measurements, the case having illuminated area equals to 15.6 cm^2 is considered as the representative of the experimental results as the impacts of the illuminated area in this case are negligible. From this figure it is concluded that the changes in the efficiency due to increasing the light intensity from 0.7 sun to 1 sun are minor in both COMSOL and theory therefore in the experimental results, the changes are negligible. For light intensities more than 1 sun, the comparison between COMSOL and theory is previously presented in section 2.6 which verifies the accuracy of the COMSOL model. However, it is not possible to use other values of the illumination to further validate the simulations. This is due to the limitations of the experimental setup, which does not allow the creation of uniform concentrated illumination.

4.3 Effects of the temperature

As discussed in sections 2.7 and 3.3, increasing the temperature leads to drop in the efficiency. To validate the simulated model, the efficiency of the cell in 25 ˚C and 40 ˚C are plotted based on the results derived from COMSOL, the experiments and the theory and is shown in Figure 4.2. Both simulation results and measurements show a reduction in the efficiency of around 0.06 and 0.05 when increasing the temperature from 25 ˚C to 40 ˚C which is in good agreement with the theory that predicts a 0.04 decrease in the normalized efficiency. This validates the accuracy of the simulated model in predicting the impacts of temperature on the efficiency of the cell.
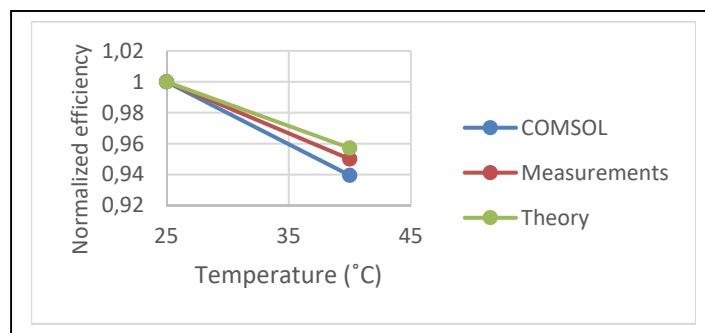
Figure 4.2 Temperature's effect on the efficiency
based on simulated model, experiments and theory

4.4   Effects of non-uniform illumination

As the main purpose of this thesis is to study the impacts of non-homogenous illumination on the efficiency of the cell, the results obtained from the simulation and measurements for non-uniform illumination should be analyzed to determine the accuracy of the simulated model. Regarding the simulations, the Gaussian profiles were selected as case studies due to the frequent occurrence in the trough concentrator systems. In the case of the experiments, due to the setup, the illumination profiles were not perfectly Gaussian. Figure 4.3 illustrates the illumination patterns which were studied in 1 sun illumination while having focus point illumination as well as the selected area of the illumination grid as the case studies.
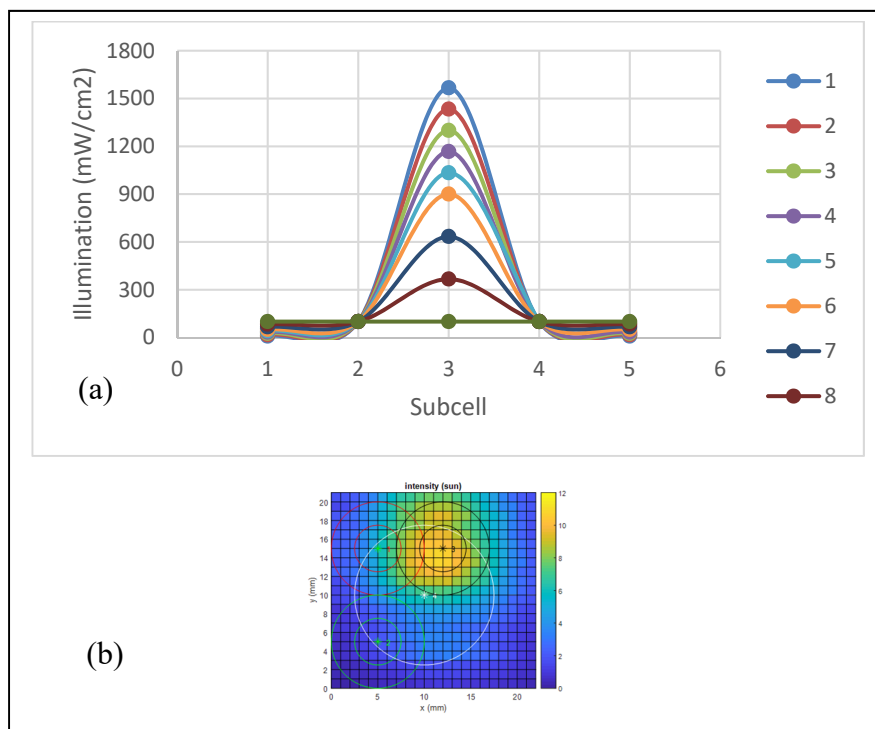
Figure 4.3 Illumination patterns in (a) simulations (b) experiments

The results obtained from both simulation and experiments show two different scenarios towards non-uniformity. The first scenario occurs while having lower light intensity which prevents reaching the saturation and the second one happens when the light intensity is high enough that saturation occurs. The light intensity at which the saturation happens is dependent

on the illuminated area. It should be noted that a smaller illuminated area leads to a reduction of the light intensity at which the saturation happens. Therefore, the effects of non-uniform illumination on the efficiency are normalized and studied before and after saturation.

4.4.1   Before saturation

In simulation chapter, section 2.8. the model is studied having different perfectly Gaussian illumination profiles to check the effects of non-uniformity on the efficiency of the solar cell. In low concentration, the results show better performance of the model while having higher non-uniformity factor along the cell. On the other hand, in the experiments due to the limitations of the setup, the illumination profiles are not perfectly Gaussian. However, the results show better performance of the cell in lower light intensities while having a non-uniform illumination rather than the uniform profile. In order to validate the results of the simulations and measurements, the normalized efficiency for non-uniform illumination for both COMSOL and experiments are plotted and shown in Figure 4.4. For the experimental results, the case 4 is selected as the representative of the experiments before occurrence of the saturation. This is the case having aperture of 0.79 cm^2 and average illumination of 2 sun. The r-factor for this case is 2.65 which shows severe non-uniformity. The low average illumination over the cell in this case prevents the occurrence of saturation despite the small illuminated area.
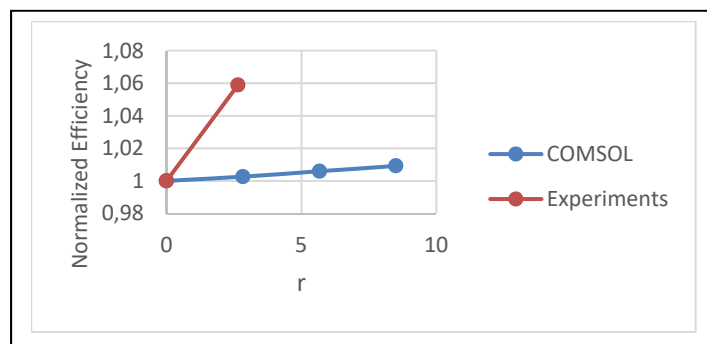

Figure 4.4 Efficiency changes versus non-uniformity
in simulation and measurements in relatively low
concentration illumination

As it is shown in the Figure 4.4, the efficiency sees minor increase by having higher non-uniformity factor. However, for the experimental results, these changes are more considerable which can be explained as the simulated model is a simplification of the reality and does not take fully account of all the complex phenomena. Moreover, the simulated illumination profiles are perfectly Gaussian, while in the experiments the illumination pattern is not perfectly Gaussian.

4.4.2   After saturation

The results obtained from simulation in section 2.8 for high concentration show the severe impacts of the non-uniformity on the performance of the cell. This is due to the saturation which occurs in higher light intensities. On the other hand, in the measurements for the cases having higher average illumination over the cell, the non-uniformity leads to poor performance of the cell. As an illustration, the case 5 is chosen to present experimental results as the average illumination is 9.64 sun over illuminated area of 0.79 cm^2. In order to compare the results obtained from simulations and measurements, the efficiency is normalized and plotted for both measurements and simulations and shown in Figure 4.5. When the average light intensity is high enough that the saturation happens, both measurements and simulation show a decrease in the efficiency due to the non-uniform illumination. This decrease is more considerable while having higher degrees of non-uniformity. In general, the effects of the non-uniformity on the efficiency in the experiments are more considerable than having the same non-uniformity factor in the simulation. This happens as the simulation does not take into account all the aspects and complexity of the real cell. Moreover, the intensity at which the non-uniformity of the illumination reduces the performance of the solar cell is different for the simulation and measurement. This intensity is greater in the case of the simulation than in the experimental measurements. This can be attributed to the small illuminated area and the severe shading over the cell in the experiments.
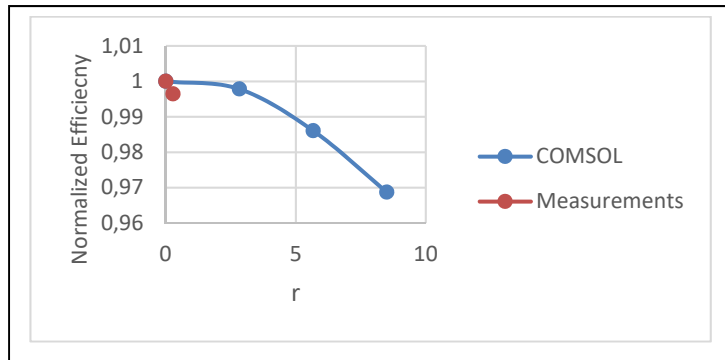
Figure 4.5 Efficiency changes versus non-uniformity in
simulation and measurements in relatively high
concentration illumination

Generally, the results of the experiments show the same trend as the COMSOL model towards non-uniformity in both lower and higher light intensities which verifies the accuracy of the COMSOL model to predict the behavior of the solar cell under non-uniform illumination.

4.5   Conclusion

In this chapter the correlation between simulation and experiments is studied in three different aspects of the light intensity, temperature and non-uniformity factor. The results confirmed the validity of the COMSOL simulation in modeling the solar cell under different conditions. Considering the effects of the concentrated illumination on the efficiency of the solar cell, both simulation and measurements showed slight increase in the efficiency by having higher light intensity which is accurate based on the theory. In the case of, the temperature effects on the efficiency of the solar cell simulation results and experimental results were compared. Both were in good agreement with the theory, as the efficiency reduces when the temperature rises.

Regarding the non-uniform illumination, the results were analyzed in two cases of before occurrence of saturation and after saturation happens. Both simulation and experiments show the same behavior towards non-uniformity in these two cases. However, the saturation happens at lower light intensities in experiments than the simulation, which is due to the large shading

over the cell in experiments as well as the simplicity of the simulated model which does not contain all the complex aspects of the solar cell.

CONCLUSION

In this thesis, a Silicon back-contact solar cell has been modeled and analyzed using COMSOL, which showed a good agreement with the SunPower back-contact solar cell under 1 sun illumination. The model was studied having different doping for each region and the related Voc, Jsc and efficiency was extracted to study the effects of the doping on the performance of the cell. To verify the model, the results obtained from simulations were compared with theory, using Matlab which showed a good agreement between the parameters of the modeled cell and the expected parameters from theory, under different degrees of concentrated light. Moreover, the impacts of the temperature on the efficiency of the simulated model were studied which showed a good agreement with the literature.

The non-uniformity factor (r) was presented as the indicator of non-uniformity for illumination profiles. The efficiency of the model was calculated under different illumination from 1 sun to 300 sun for Gaussian non-uniform illumination profiles and the results were analyzed considering non-uniformity factor. The illumination profiles were applied in three different cases, assuming the non-uniformity along the metal contacts, across the metal contacts and 2D non-uniform pattern that had the most illuminated point on the center of the model.

The results of simulations showed minor improvements in the performance of the cell while having non-uniform illumination in low concentration. For low concentration, the sharper the Gaussian profile was, the better performance was achieved. Regarding high concentration, as it is the case for 300 sun, due to the saturation, the best performance happened while having uniform illumination over the cell. In this case, by increasing the non-uniformity the efficiency of the simulated model drops considerably.

Considering all, the simulations showed slight improvements in the efficiency while having non-uniform illumination in low concentration. However, the effects of temperature were not taken into account and it was assumed that the ideal cooling system kept the temperature steady around 25 ˚C.

To verify the results obtained from the simulation, the sample solar cell has been characterized using 2 different solar simulators in ETS and UQAM which showed the proper performance of the solar simulator used in ETS as well as the results. A black box having different apertures was proposed to achieve partial illumination on the solar cell and the effects of illuminated area has been studied.

The light beam was concentrated using a lens to get non-uniform concentrated light and the exact pattern of non-uniform illumination was measured using a photodiode, with steps of 1 mm for an area around 2 cm by 2 cm. Based on the illumination grid, 7 different cases study was selected and the parameters of the solar cell was measured for each case. The results obtained from measurements were compared with the results expected from theory, considering reference parameters which are previously measured under 1 sun uniform illumination. Due to the effects of the temperature on the characteristics of the solar cell, the temperature was monitored during experiments using thermocouple and its impact on the characteristics of the cell were applied based on the temperature coefficients.

The results of measurements showed better performance while having non-uniform illumination in cases having lower concentrations. The best performance of the cell occurred having average 6 sun illumination over the cell. For cases having higher average illumination, due to the small illuminated area, the saturation happened which led to lower efficiency. For these cases, the best efficiency happened while having uniform illumination.

As a summary, it can be concluded that the non-uniform illumination can lead to better performance of the cell in low concentration when the temperature stays around 25 ˚C. However, in higher concentration ratios, the non-uniformity results in a drop in the efficiency of the cell.

Future work on this subject can be first of all improving the simulated model by optimizing the dimensions and the doping of the solar cell. Moreover, studying the effects of non-uniform illumination using other types of solar cells as well as creating optimal non-uniform

illumination patterns using masks to verify the results obtained from simulations are of great interest. Regarding the influence of the temperature, analyzing different temperature profiles along the cell is of great value as it is the case in most of the concentrated solar cell systems.

DATASHEET

MAXEON™ GEN III SOLAR CELLS

Electrical Characteristics of a typical Maxeon Gen III Cell At Standard Test Conditions (STC)
STC: 1000W/m², AM 1.5G and cell temp 25°C

	Cell Bin	Pmpp (Wp)	Eff. (%)	Vmpp (V)	Impp (A)	Voc (V)	Isc (A)
Ultra Peak Performance	Me1	3.72	24.3	0.632	5.89	0.730	6.18
Ultra Premium Performance	Le1	3.63	23.7	0.621	5.84	0.721	6.15
Ultra High Performance	Ke1	3.54	23.1	0.612	5.79	0.713	6.11

Electrical parameters are nominal values.
Temp.Coefficients in SunPower Panels: Voltage: -1.74mV/°C, Current: 2.9mA/°C, Power: -0.29%/°C

Spectral Response

References
SunPower: NREL data, commissioned by SPWR
Conventional: Progress in Photovoltaics: Research and Applications, Solar cell efficiency tables, version 36 18(5), (2010) 46-352
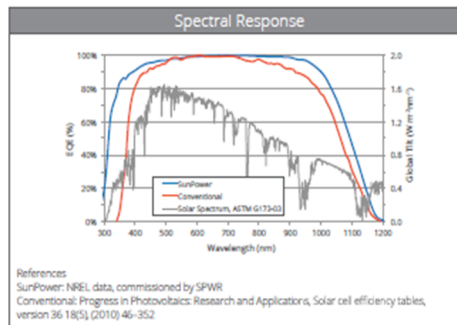
Cell Physical Characteristics

Wafer:	Monocrystalline silicon
Design:	All back contact
Front:	Uniform, black antireflection coating
Back:	Tin-coated, copper metal grid
Cell Area:	Approximately 153cm²
Cell Weight:	Approximately 6.5grams
Cell Thickness:	150μm +/- 30μm

Bond pad detail with positive indicator

5.4

Positive Bond Pads

125
3.0 3.0
125
160
38.5 38.5

Dimensions in mm

Bond pad area dimensions are 5.4mm x 3.0mm
Metal finger pitch between positive and negative fingers is 471um.
Positive/Negative pole bond pad sides have "+/-" indicators on leftmost and rightmost bond pads
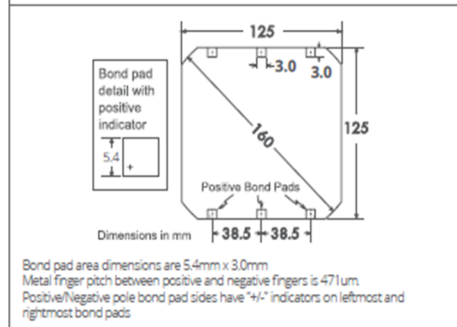
Positive Electrical Grounding

If cell voltage is below frame ground the cell power output will be reduced. Therefore, modules and systems produced using these cells should be configured as "positive ground systems." If this creates a problem, please consult with SunPower.

Interconnect Tab and Process Recommendations

SunPower recommends customers use SunPower's patented tin-plated copper strain-relieved interconnect tabs, which can be purchased from SunPower. These interconnects are easily solderable and compatible with lead free processing. Tabs weigh approximately 0.3 grams.

Our patented interconnect tabs are packaged in boxes of 3600 or 36,000 each.

http://us.sunpower.com/about/sunpower-technology/patents/

Production Quality

ISO 9001:2015 certified

Soft handling procedures to reduce breakage and crack formation

100% cell performance testing and visual inspection

Packaging

Cells are packed in boxes of 1500 each; grouped in 10 shrink-wrapped stacks of 150 with interleaving. 24 boxes are packed in a water-resistant "Master Carton" containing 36,000 cells suitable for air transport.

Purchase Terms

Customers shall not reverse engineer, disassemble or analyze the Solar Cells or any prototype, process, product, or other item that embodies Confidential Information of SunPower. Customers shall not cause or allow any inspection, analysis, or characterization of any properties (whether mechanical, structural, chemical, electrical, or otherwise) of the Solar Cells, whether by itself or by a third party.

Customer agrees that it will not transfer (whether by sale, loan, gift, or other conveyance) the Solar Cells from its possession.

SunPower solar cells are provided "AS IS" without warranty.

Full terms and conditions are in the Cell Purchase Agreement

SUNPOWER

Figure-A I 1 Datasheet of Maxeon GEN III solar cell, (SUNPOWER)

LIST OF BIBLIOGRAPHICAL REFERENCES

Alharbi, Fahhad H. et Sabre Kais. 2015. *Theoretical limits of photovoltaics efficiency and possible improvements by intuitive approaches learned from photosynthesis and quantum coherence. Renew. Sustain. Energy Rev.* <https://doi.org/10.1016/j.rser.2014.11.101>.

Baharoon, Dhyia Aidroos, Hasimah Abdul Rahman, Wan Zaidi Wan Omar et Saeed Obaid Fadhl. 2015. « Historical development of concentrating solar power technologies to generate clean electricity efficiently – A review ». *Renewable and Sustainable Energy Reviews*, vol. 41, p. 996–1027. <https://doi.org/10.1016/j.rser.2014.09.008>.

Basit, A, M u Rehman, J Aziz et A A Malik. 2014. « Design and fabrication of parabolic trough solar energy system ». In *2014 International Conference on Energy Systems and Policies (ICESP)*. (2014), p. 1–8. <https://doi.org/10.1109/ICESP.2014.7346988>.

Belkassmi, Y, A Rafiki, K Gueraoui, L Elmaimouni, O Tata et N Hassanain. 2017. « Modeling and simulation of photovoltaic module based on one diode model using Matlab/Simulink ». In *2017 International Conference on Engineering MIS (ICEMIS)*. (2017), p. 1–6. <https://doi.org/10.1109/ICEMIS.2017.8272965>.

Coventry, Joe S. 2005. « Performance of a concentrating photovoltaic/thermal solar collector ».*Solar Energy*, vol. 78, nᵒ 2, p. 211–222. <https://doi.org/10.1016/j.solener.2004.03.014>.

Fell, Andreas, Kean C. Fong, Keith R. McIntosh, Evan Franklin et Andrew W. Blakers. 2014. « 3-D simulation of interdigitated-back-contact silicon solar cells with Quokka including perimeter losses ». *IEEE Journal of Photovoltaics*, vol. 4, nᵒ 4, p. 1040-1045. <https://doi.org/10.1109/JPHOTOV.2014.2320302>.

Green, Martin A., Ewan D. Dunlop, Jochen Hohl-Ebinger, Masahiro Yoshita, Nikos Kopidakis et Anita W.Y. Ho-Baillie. 2020. « Solar cell efficiency tables (Version 55) ». *Progress in Photovoltaics: Research and Applications*, vol. 28, nᵒ 1, p. 3-15. <https://doi.org/10.1002/pip.3228>. Consulté le 16 mars 2020.

Hamel, A. 2016. « Improvement of quantum efficiency using surface texture of solar cell in the form of pyramid ». *Physics of Particles and Nuclei Letters*, vol. 13, nᵒ 1, p. 69–73. <https://doi.org/10.1134/S1547477116010106>.

Herrero, Rebeca, Marta Victoria, César Domínguez, Stephen Askins, Ignacio Antón et Gabriel Sala. 2012. « Concentration photovoltaic optical system irradiance distribution measurements and its effect on multi-junction solar cells ». *Progress in Photovoltaics: Research and Applications*, vol. 20, nᵒ 4, p. 423–430. <https://doi.org/10.1002/pip.1145>.

Hosenuzzaman, M, N A Rahim, J Selvaraj, M Hasanuzzaman, A B M A Malek et A Nahar. 2015. « Global prospects, progress, policies, and environmental impact of solar photovoltaic power generation ». *Renewable and Sustainable Energy Reviews*, vol. 41, p. 284-297. <https://doi.org/10.1016/j.rser.2014.08.046>.

Jazayeri, M, S Uysal et K Jazayeri. 2013. « A simple MATLAB/Simulink simulation for PV modules based on one-diode model ». In *2013 High Capacity Optical Networks and Emerging/Enabling Technologies*. (2013), p. 44–50. <https://doi.org/10.1109/HONET.2013.6729755>.

Jooss, W., H. Knauss, F. Huster, P. Fath, E. Bucher, R. Tölle et T. M. Bruton. 2000. « Back contact buried contact solar cells with metallization wrap around electrodes ». In *Conference Record of the IEEE Photovoltaic Specialists Conference*. (2000), p. 176-179. Institute of Electrical and Electronics Engineers Inc. <https://doi.org/10.1109/PVSC.2000.915783>.

Kerschaver, Emmanuel Van et Guy Beaucarne. 2006. « Back-contact solar cells: a review ». *Progress in Photovoltaics: Research and Applications*, vol. 14, nº 2, p. 107–123. <https://doi.org/10.1002/pip.657>.

Van Kerschaver, Emmanuel, S. De Wolf et J. Szlufcik. 2000. « Towards back contact silicon solar cells with screen printed metallisation ». In *Conference Record of the IEEE Photovoltaic Specialists Conference*. (2000), p. 209-212. Institute of Electrical and Electronics Engineers Inc. <https://doi.org/10.1109/PVSC.2000.915791>.

Khamooshi, Mehrdad, Hana Salati, Fuat Egelioglu, Ali Hooshyar Faghiri, Judy Tarabishi et Saeed Babadi. 2014. *A Review of Solar Photovoltaic Concentrators*. <https://www.hindawi.com/journals/ijp/2014/958521/abs/>.

Lammert, M D et R J Schwartz. 1977. « The interdigitated back contact solar cell: A silicon solar cell for use in concentrated sunlight ». *IEEE Transactions on Electron Devices*, vol. 24, nº 4, p. 337–342. <https://doi.org/10.1109/T-ED.1977.18738>.

Languy, Fabian et Serge Habraken. 2013. « Nonimaging achromatic shaped Fresnel lenses for ultrahigh solar concentration ». *Optics Letters*, vol. 38, nº 10, p. 1730-1732. <https://doi.org/10.1364/OL.38.001730>.

Li, Guiqiang, Qingdong Xuan, Gang Pei, Yuehong Su et Jie Ji. 2018. « Effect of non-uniform illumination and temperature distribution on concentrating solar cell - A review ». *Energy*, vol. 144, p. 1119–1136. <https://doi.org/10.1016/j.energy.2017.12.067>.

López Rodríguez, Gema. 2016. *Interdigitated Back-contacted(IBC) c-Si solar cells based on laser processed dielectric layers*.

Luque, A, G Sala et J C Arboiro. 1998. « Electric and thermal model for non-uniformly illuminated concentration cells ». *Solar Energy Materials and Solar Cells*, vol. 51, nº 3, p. 269–290. <https://doi.org/10.1016/S0927-0248(97)00228-6>.

Al Mamun, Mohammad Abdullah, Md Hasanuzzaman et Jeyraj Selvaraj. 2017. « Experimental investigation of the effect of partial shading on photovoltaic performance ». *IET Renewable Power Generation*, vol. 11, nº 7, p. 912-921. <https://doi.org/10.1049/iet-rpg.2016.0902>.

Mat Desa, M K, S Sapeai, A W Azhari, K Sopian, M Y Sulaiman, N Amin et S H Zaidi. 2016. « Silicon back contact solar cell configuration: A pathway towards higher efficiency ». *Renewable and Sustainable Energy Reviews*, vol. 60, p. 1516-1532. <https://doi.org/10.1016/j.rser.2016.03.004>.

Mellor, A, J L Domenech-Garret, D Chemisana et J I Rosell. 2009. « A two-dimensional finite element model of front surface current flow in cells under non-uniform, concentrated illumination ». *Solar Energy*, vol. 83, nº 9, p. 1459–1465. <https://doi.org/10.1016/j.solener.2009.03.016>.

Moraitis, P, R E I Schropp et W G J H M van Sark. 2018. « Nanoparticles for Luminescent Solar Concentrators - A review ». *Optical Materials*, vol. 84, p. 636–645. <https://doi.org/10.1016/j.optmat.2018.07.034>.

Murphree, Quincy C. 2001. « A point focusing double parabolic trough concentrator ». *Solar Energy*, vol. 70, nº 2, p. 85–94. <https://doi.org/10.1016/S0038-092X(00)00138-9>.

Pan, Jui-Wen, Jiun-Yang Huang, Chih-Ming Wang, Hwen-Fen Hong et Yi-Ping Liang. 2011. « High concentration and homogenized Fresnel lens without secondary optics element ». *Optics Communications*, vol. 284, nº 19, p. 4283–4288. <https://doi.org/10.1016/j.optcom.2011.06.019>.

Paul, Damasen Ikwaba, Mervyn Smyth, Aggelos Zacharopoulos et Jayanta Mondol. 2015. *The Effects of Nonuniform Illumination on the Electrical Performance of a Single Conventional Photovoltaic Cell*. <https://www.hindawi.com/journals/ijp/2015/631953/>.

Pérez-Higueras, P., E. Muñoz, G. Almonacid et P. G. Vidal. 2011. *High Concentrator PhotoVoltaics efficiencies: Present status and forecast. Renew. Sustain. Energy Rev.* <https://doi.org/10.1016/j.rser.2010.11.046>.

Pfeiffer, H et M Bihler. 1982. « The effects of non-uniform illumination of solar cells with concentrated light ». *Solar Cells*, vol. 5, nº 3, p. 293–299. <https://doi.org/10.1016/0379-6787(82)90045-X>.

Reis, F, C Guerreiro, F Batista, T Pimentel, M Pravettoni, J Wemans, G Sorasio et M C Brito. 2015. « Modeling the Effects of Inhomogeneous Irradiation and Temperature Profile on CPV Solar Cell Behavior ». *IEEE Journal of Photovoltaics*, vol. 5, nº 1, p. 112-122. <https://doi.org/10.1109/JPHOTOV.2014.2358080>.

Shanks, Katie, S Senthilarasu et Tapas K Mallick. 2016. « Optics for concentrating photovoltaics: Trends, limits and opportunities for materials and design ». *Renewable and Sustainable Energy Reviews*, vol. 60, p. 394–407. <https://doi.org/10.1016/j.rser.2016.01.089>.

Sharma, Pratibha. 2017. « Modeling, Optimization, and Characterization of High Concentration Photovoltaic Systems Using Multijunction Solar Cells ». Université d'Ottawa / University of Ottawa. <http://ruor.uottawa.ca/handle/10393/35917>.

Zeman, Miro. [s d]. « INTRODUCTION TO PHOTOVOLTAIC SOLAR ENERGY ». In *SOLAR CELLS*. <http://mikro.elfak.ni.ac.rs/wp-content/uploads/Solar-Cells-Miro-Zeman.pdf>.